AMR Seminar #78 – Short Summary of Cases:

Case 1: F.50 with right knee mass.

Case 2: M.72 with history of HepC cirrhosis, now presents with a 3.6 cm nodule in the liver.

Case 3: M.77 presented with a 6.0 cm painful subcutaneous mass in his right buttock that had been "slowly growing over many years".

Case 4: F.42 was seen in consultation for abnormal uterine bleeding of 8 months' duration.

Case 5: F.6 presented with a retroperitoneal lesion.

Case 6: F.70 presented with an enlarging thyroid mass.

Case 7: F.63 complained of a palpable mass in the axilla.

Case 8: F.62 presented with an 8 cm esophageal mass involving all layers of her esophagus and abutting her aorta.

Case 9: M.61 presented with an old-standing ulcerated lesion involving the right cheek.

Case 10: F.41 presented with a right buttock mass of unknown duration.

Case 11: F.32 presented with hydronephrosis; imaging revealed 8.5 cm renal mass in the left kidney.

Case 12: F.52 was seen for a 2.5 cm left ovarian mass.

Case 13: A 6-weeks-old female patient presented with a large, pigmented lesion at the back of her head.

Case 14: F.50 presents with a 2.5 cm partly solid infiltrate peripherally in right lower lobe on chest CT scan.

Case 15: M.69, on CT scan revealed a 6 cm mass in the anterior mediastinum, highly suspicious for thymoma.

Case 16: F.32 presents with a 3.9 x 3.6 x 2.2 cm subcutaneous mass in the left inguinal region.

Case 17: F.28 with multinodular goiter.

Case 18: F.52 with 17 cm. left ovarian mass.

Case 19: F.62 with abnormal uterine bleeding and 12 cm. right ovarian mass.

AMR SEMINAR #78
CASE 1

Contributed by: Kum Cooper, University of Pennsylvania.

Clinical History: 50 year woman with history of right knee mass, clinically and radiologically consistent with PVNS. Soft tissue tumor mass measured 6.5 x 4.9 x 2.7 cm, well circumscribed with pale yellow cut surface. No hemorrhage nor necrosis. Tumor cells positive for CD34 and D2-40 (weak), histiocytes positive for CD163.

Diagnosis: Myxoinflammatory fibroblastic sarcoma (MIFS).

Discussion: The first case of MIFS I saw in the early 2000s was presented to this group. That case was subsequently added to a series written up in 2002 by Dr Lamovec (our good friend from Ljubljana along with Saul), who drew attention to the proximal location of these tumors (until then the prefix "acral" preceded MIFS). First described in 1998 by three different groups (including our good friend Michal Michal), the WHO eventually settled on a single diagnostic terminology MIFS.

This tumor has had a very interesting and controversial evolution with t(1;10) TGFBR3/MGEA5 being at the center of the relationship between hemosiderotic fibrolipomatous tumor (HFLT) and pleomorphic hyalinizing tumor (PHAT); reviewed in Arch Pathol, 143; 2019.
The submitted case proved to be clinically and radiologically challenging since PVNS (TSGCT) was the favored diagnosis, primarily due to the location and the radiological interpretation/imaging.

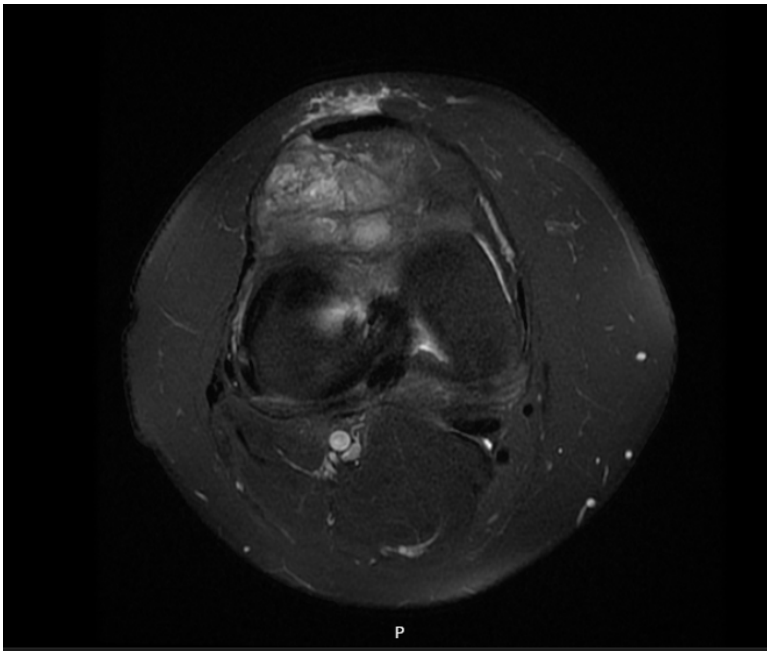
P

AMR SEMINAR #78
CASE 2

Contributed by: Alberto Cavazza, M.D. (with the collaboration of Dr. Giacomo Santandrea), Italy.

Clinical History: The patient was a 72-year old man, with Hep C virus-related cirrhosis, presenting with a hyperechogenic lesion located in the IV segment of the liver. A CT-scan showed a 10 mm hyperdense nodule adjacent to a 26 mm hypodense lesion: the radiological picture was consistent with a small HCC surrounded by a fibrotic area. The patient underwent a fine needle biopsy, that was nondiagnostic, so the lesion was surgically excised.
Gross examination of the resected liver parenchyma revealed a 1 cm yellowish solid nodule merging into a surrounding 3 cm firm white area.

Pathologic Findings: Histologically, the nodule was characterized by a proliferation of mildly atypical epithelioid cells with coarse chromatin, scant nucleoli, occasional nuclear pseudoinclusions and abundant eosinophilic cytoplasm, arranged in trabeculae and acini. The surrounding white area consisted in interconnected cords of fusiform and epithelioid cells with mild atypia, focally forming small vessels, embedded in a dense fibrous stroma infiltrating among ductular structures and extending into the wall of several medium-sized vessels, with occlusion of their lumen. In the border of your slide there is a residue of liver parenchyma with cirrhosis. By immunohistochemistry, the nodule was positive for Glutamine Synthetase, Glypican-3, keratin CAM 5.2 and keratin 7, whereas the surrounding lesion showed expression for CD31, CD34, ERG, D2-40, with focal positivity for keratin CAM 5.2 and keratin 7. Pan-keratin and ALK were negative. No molecular analysis was performed.

Diagnosis: (Initial diagnosis) Hepatocellular carcinoma associated with epithelioid hemangioendothelioma of the liver.

Discussion: The combination of hepatocellular carcinoma and epithelioid hemangioendothelioma in the same liver nodule seems to be very rare; we were able to find only a single case reported in the literature (Athanasopoulos et al. Medicine. 2015;94(34):e1377).

However, in reviewing the case for this seminar, I started to have doubts on the correctness of my original diagnosis. In particular, I became convinced that the hemangioendothelioma component of the diagnosis was wrong: in retrospect, morphology was at least not classical and immunostains were at least borderline. I still thought it was malignant, but I did not know what it was, so I sent the case to an expert in soft tissues. He excluded an epithelioid hemangioendothelioma (CAMTA1 was negative), and he interpreted the tissue surrounding the hepatocellular carcinoma as ischemic/reactive in nature, secondary to the thrombotic vascular occlusions. After 1 year from surgery, the patient presented with jaundice due to local progression of the disease and with multiple bone metastases. Nothing else was found elsewhere.

A vertebral biopsy showed a focal localization of atypical spindle cells that were positive for pan-keratin, quite similar to the cells present in the liver (see pictures below).

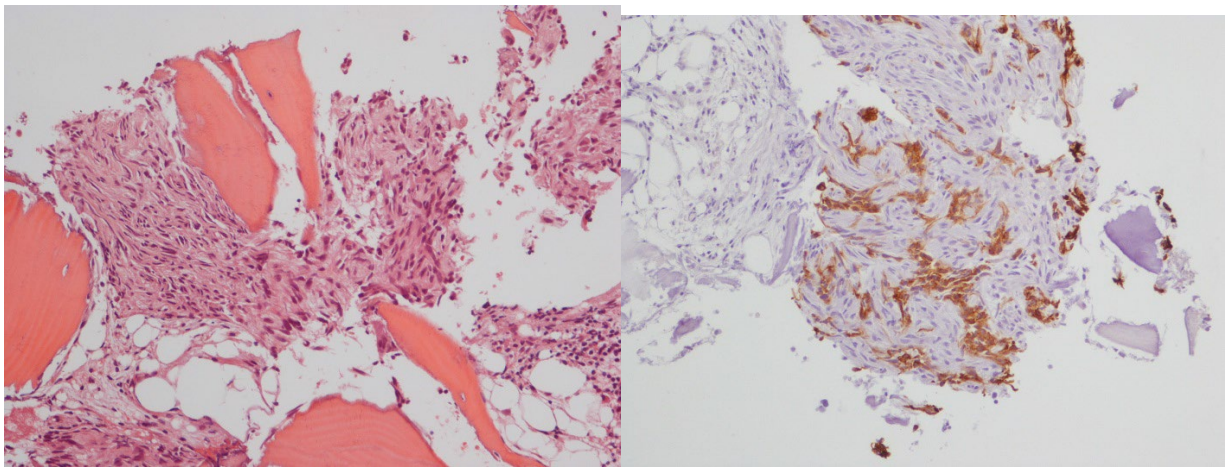

I performed pan-keratin on different blocks on the previous liver excision, and I found a multifocal positivity (see below).

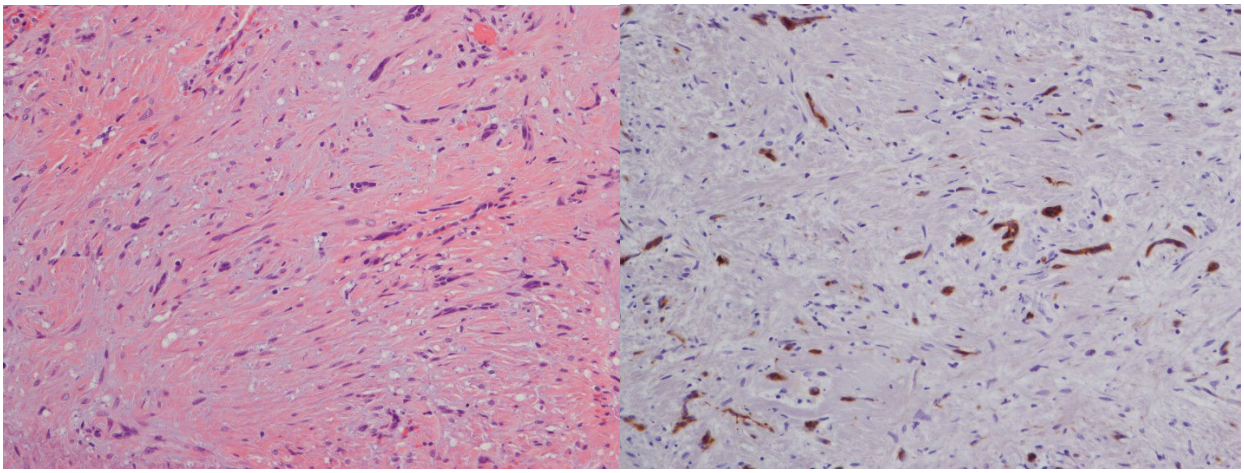

In the end, I think the lesion is a **sarcomatoid carcinoma of the liver**, maybe arisen as a dedifferentiation of the hepatocellular carcinoma (?) and with bone metastases. In retrospect, I think the vascular invasions seen in the liver is identical to what can be seen in occasional sarcomatoid carcinomas of the lung, deceptively bland and sometimes masqueraded by secondary infarcts. The patient is still alive with progressive disease in spite of chemotherapy. I apologize for my mistake and for the confusion of this presentation, but I thought it was more correct (and maybe interesting) to document it as it really happened. Your opinions and comments will be very appreciated.

AMR SEMINAR #78
CASE 3

Contributed by: Brandon Larsen, M.D., Ph.D., Mayo Clinic, Scottsdale.

Clinical History: A 77-year-old man presented with a 6.0 cm painful subcutaneous mass in his right buttock that had been "slowly growing over many years". Further details and imaging studies were unavailable, but the surgeon favored a benign cyst, and a local excision was performed. The primary pathologist initially favored undifferentiated pleomorphic sarcoma but decided to send the case to our institution for a second opinion.

Pathologic Findings: The sections show a relatively well-circumscribed proliferation of markedly atypical and frankly bizarre pleomorphic fibroblastic spindle cells with abundant eosinophilic "glassy" cytoplasm. Abundant hemosiderin-laden macrophages are also present. Within the central portion of the tumor is an area of organizing hematoma formation. Despite its striking cytologic atypia, the tumor is essentially devoid of mitotic activity and necrosis is absent. Immunohistochemistry showed strong and diffuse positive staining of the tumor for CD34 and focal weak staining for AE1/AE3, but no staining for CD31, ERG, HMW-cytokeratin, pancytokeratin, CK8/18, SOX10, melan-A, S100 protein, melan-A, desmin, or myogenin.

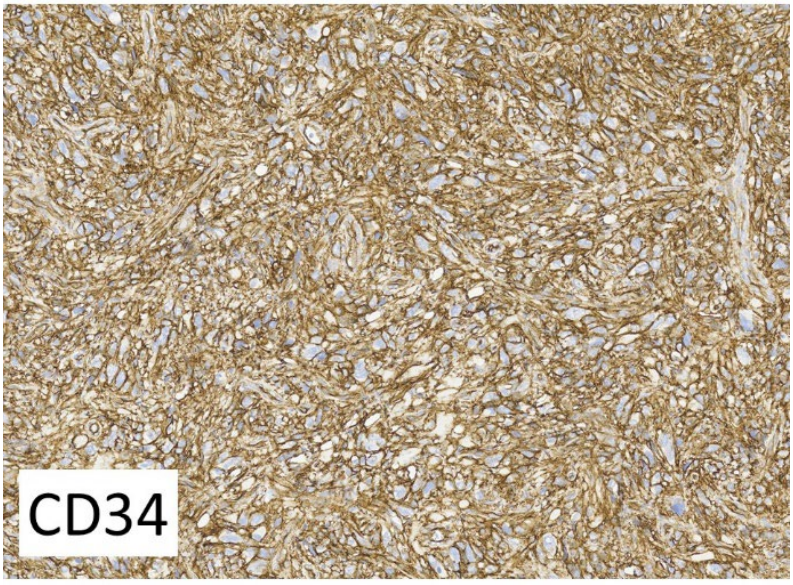

Diagnosis: Superficial CD34-positive fibroblastic tumor.

Comment: Superficial CD34-positive fibroblastic tumor is a rare low-grade fibroblastic neoplasm that was first recognized as a distinct entity in 2014 by Dr. Andrew Folpe (a prior

AMR member) and colleagues at Mayo Clinic and Emory, who published the first series of 18 cases of this tumor at that time. A second series of 11 cases from China was published in 2017, but this tumor remains poorly understood and to date, less than 40 cases have been reported in the literature. This entity was recently added to the updated 5th Edition of the WHO Classification of Tumours of Soft Tissue and Bone, released in 2020. Hopefully this formal recognition by the WHO will increase recognition of this rare entity.

Based on the published literature, it seems that this tumor usually arises in the subcutaneous tissues of the thigh, buttock, or arm, but can also arise in the shoulder, vulva, or other sites. Most tumors occur in middle-aged adults, though the reported age range is broad, as the current case illustrates. The molecular biology of these tumors remains poorly understood, though rearrangements of the PRDM10 gene have been reported in 3 cases. No molecular analysis was performed in the present case. From published data, it seems that the prognosis is excellent. Even at first glance, it is easy to see how this tumor can be misdiagnosed as undifferentiated pleomorphic sarcoma or some other high-grade sarcoma (many of those cells are ugly!), yet the clinical history provides important clues suggesting a low-grade or indolent neoplasm, rather than a high-grade malignancy, as does the disproportionate lack of mitotic activity relative to the striking cytologic atypia present.

As often occurs in pathology practice, I imagine the most challenging aspect of this diagnosis is simply being aware that the entity exists and thinking of the possibility in the first place. I found this to be a quite lovely example of this very rare tumor and thought the AMR Club would appreciate seeing it as well. It is also interesting that the tumor contains an area of organizing hematoma formation, which I suspect was from prior traumatic injury to the area and the likely cause of pain that brought this patient to clinical attention (pain is not a typical complaint in most cases). For those of you who are curious… the answer is "yes", I did share this case with Andrew Folpe before I signed out my report, as we are both in the Mayo system and I have only encountered this tumor once before. I'm glad he was willing to review the case. I won't pretend to be an expert on this tumor, but Dr. Folpe is… and he agreed that this is a fine example of this entity, too. I hope you enjoy it.

References:

1. Carter JM, Weiss SW, Linos K, DiCaudo DJ, Folpe AL. Superficial CD34-positive fibroblastic tumor: report of 18 cases of a distinctive low-grade mesenchymal neoplasm of intermediate (borderline) malignancy. Mod Pathol. 2014;27:294-302.
2. Lao IW, Yu L, Wang J. Superficial CD34-positive fibroblastic tumor: a clinicopathological and immunohistochemical study of an additional series. Histopathology. 2017;70:394-401.
3. Rekhi B, Folpe AL, Yu L. Superficial CD34-positive fibroblastic tumor. In: WHO Classification of Tumours: Soft Tissue and Bone Tumours, 5th Ed., 2020; pp.114-5.

AMR SEMINAR #78
CASE 4

Contributed by: Delia Perez-Montiel, M.D., National Cancer Institute, Mexico.

Clinical History: A 42 year old woman was seen in consultation for abnormal uterine bleeding of 8 months' duration. Serum tumor markers were negative.

Pathologic Findings: The case was referred to us from another institution. The pathology report indicated that, grossly, there were multiple intramural and sub mucosal nodules, the largest one measured 5.6 cm, was well delimited, light yellow (the slide that your received is from this lesion). The rest of the nodules were white, firm, with a leiomyomatous appearance. The endometrial cavity and cervix were normal. We requested the original specimen; multiple fragments of uterus were received, and additional sections were taken.

The lesion had well delimited borders; the cells were monotonous small, polygonal with eosinophilic cytoplasm, round to oval nuclei, with diffuse open chromatin, with some trabecular, ribbon-like and "pseudoalveolar" areas. The stroma in some areas was myxoid and had scant extracellular matrix. Thick- walled vessels were present. No atypical mitoses, necrosis or vascular invasion were seen. Endometrium and cervix were unremarkable. By immunohistochemistry, the tumor cells were positive to actin and H caldesmon, negative to CD10, CyclinD1, CK18, P16, P53, PS100, Inhibin, HMB45 and Melan A. Ki67 index was 2%. Two years after the diagnosis the patient is well, without evidence of disease.

Diagnosis: Uterine epithelioid leiomyoma.

Comment: Uterine leiomyomas are the most frequent gynecologic neoplasms, however, there are morphological variants with worrisome features. In this case, the solid and epithelioid appearance was suggestive of endometrial stromal sarcoma, but no mitosis or infiltrative margins were seen; besides immunomarkers for CD10 and cyclin D1 were negative. Epithelioid leiomyosarcoma or *STUMP* were also considered, however, no atypia, mitosis or necrosis were found.

Epithelioid leiomyoma has received other names such as leiomyoblastoma and clear cell leiomyoma, however, our case did not show extensive clear cytoplasm. In 2020 the WHO GYN pathology classification there is a brief description of this tumor as a polygonal monotonous cell with eosinophilic granular cytoplasm, similar to this tumor. Prayson et al described epithelioid uterine smooth muscle tumors, in which the cells had clear or extensive eosinophilic cytoplasmic, some of them with rhabdoid appearance. They described different nuclear grades and mitotic activity and concluded that necrosis and significant nuclear atypia predict malignancy but in contrast with usual leiomyosarcoma, mitosis are fewer in this entity (3 or 4 MF/10HPF).

References:

- Oliva, E. Practical issues in uterine pathology from banal to bewildering: the remarkable spectrum of smooth muscle neoplasia. Mod Pathol 29 (Suppl 1), S104–S120 (2016). https://doi.org/10.1038/modpathol.2015.139

- WHO Classification of Tumours Editorial Board. Female Reproductive genital tumours. Lyon (France): International Agency for Research on Cancer; 2020. (WHO classification of tumors series, 5th ed.; vol.4) https://publications.iarc.fr/592

- R A Prayson, J R Goldblum, W R Hart. Epithelioid smooth-muscle tumors of the uterus: a clinicopathologic study of 18 patients. Am J Surg Pathol. 1997 Apr;21(4):383-91. doi: 10.1097/00000478-199704000-00003.

AMR SEMINAR #78
CASE 5

Contributed by: Franco Fedeli, M.D., Malphigi Academy, Italy.

Clinical History: 6-year-old female presented with a retroperitoneal lesion.

Pathological Findings: Histologically, the neoplasm was composed mainly of hypercellular spindle cells, arranged in fascicular and herringbone patterns, closely resembling leiomyosarcoma or fibrosarcoma. The spindle cells showed oval, elongated and tapered nuclei, vesicular chromatin, inconspicuous to small nucleoli, and indistinct eosinophilic cytoplasm. The stroma was myxoid. Areas of necrosis were present.

Immunohistochemical Findings: The tumor cells were stained uniformly positive for muscle-specific actin, desmin and vimentin. Tumor cells also showed strongly positive for myogenin. The proliferative fraction, evaluated by Ki-67 (MIB-1), was 25% of the tumor cells. Other markers such as S100 protein, smooth muscle actin, cytokeratin, chromogranin, EMA, CD31, CD34, ERG, CD117 were all negative.

Molecular Findings: Evaluated with FISH, the case was negative for FKHR rearrangements.

Diagnosis: Spindle cell rhabdomyosarcoma.

Comment: Spindle cell rhabdomyosarcoma, 1 of the 3 embryonal rhabdomyosarcoma variants, was first recognized in the pediatric population in 1992 by the German-Italian Cooperative Sarcoma Study (1). The spindle cell variant is considered rare (only 3% of all RMS cases in Intergroup Rhabdomyosarcoma Study) (2). It affects mainly young males, occurs predominantly in the paratesticular region followed closely by head and neck with a minority of cases arising in other locations such as deep soft tissue of retroperitoneum and extremities. The size of these tumors can vary significantly.

Histopathology is characterized by a uniform fascicular proliferation of spindle cells with rhabdomyoblastic differentiation. The cells have centrally located nuclei with blunted or fusiform ends, small to inconspicuous or prominent nucleoli. Mitoses are easily appreciated. A small percentage of a second cell type of immature rhabdomyoblasts can be seen. Collagen fibers are frequently intermingled between the spindle cells. Our case, located in retroperitoneal region showed a prominent myxoid stroma.

Immunohistochemistry plays a fundamental role in the identification of this lesion. Spindle cell rhabdomyosarcoma regularly reacts with myogenic markers such as desmin, myogenin and MyoD1. In occasional reports, spindle cell rhabdomyosarcoma has shown variable aberrant staining for Wilms tumor1 (WT1) and CD99 (3). Rare cases with focal reactivity for keratin and EMA have been described (4)

By far the most significant distinction associated with spindle cell rhabdomyosarcoma is the prognosis. Pediatric spindle cell rhabdomyosarcoma has been shown to have a highly favorable prognosis in comparison to other forms of rhabdomyosarcoma.

References:

1) Cavazzana AO, Schmidt D, Ninfo V, et al. Spindle cell rhabdomyosarcoma: a prognostically favorable variant of rhabdomyosarcoma. Am J Surg Pathol. 1992; 16(3):229–235.

2) Newton WA Jr, Gehan EA, Webber BL, et al. Classification of rhabdomyosarcomas and related sarcomas: pathologic aspects and proposal for a new classification—an Intergroup Rhabdomyosarcoma Study. Cancer. 1995;15; 76(6):1073–1085.

3) Mentzel T, Kuhnen C. Spindle cell rhabdomyosarcoma in adults: clinicopathological and immunohistochemical analysis of seven new cases. Virchows Arch. 2006;449(5):554–560.

4) Nascimento AF, Fletcher CD. Spindle cell rhabdomyosarcoma in adults. Am J Surg Pathol. 2005;29(8):1106–1113.

AMR SEMINAR #78
CASE 6

Case contributed by: Gerald Berry, M.D., Stanford University.

Clinical History: The patient is a 70-year-old woman who presented with an enlarging thyroid mass. PET-CT imaging showed an 8 cm FDG-avid mass in the left lobe along with cervical and mediastinal adenopathy. At surgery the mass was densely adherent to and invaded the trachea and enlarged lymph nodes in the central neck and left cervical region along with extension inferiorly into the mediastinum were found. Total thyroidectomy with central and left neck lymph node dissection was performed.

Pathologic Findings: The neoplasm is composed of malignant glandular epithelium with eosinophilic cytoplasm and medium-sized nuclei with irregular outlines and variably sized central nucleoli arranged in glandular, cribriform, microcystic and sheet-like patterns. Comedo-type necrosis was present. The immunophenotypic profile: CK5/6+, CK7+, GATA3+, PAX8 subset+, mammaglobin+, thyroglobulin-, TTF1-, calcitonin-, synaptophysin-, SOX10-, S100-, BRAF V600E-. FISH testing confirmed the ETV6 gene rearrangement. Pathologic staging: pT4a, pN1a.

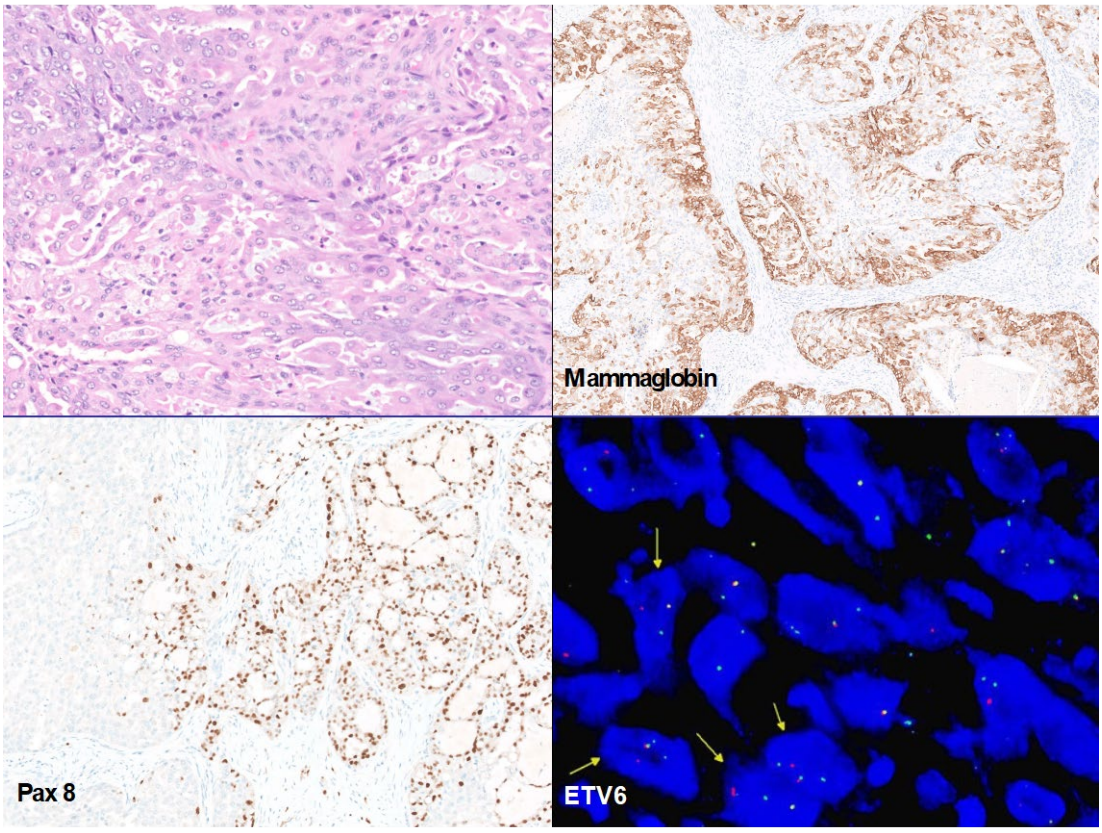

Diagnosis: Secretory (mammary analogue) carcinoma of thyroid.

Comment: I am submitting this interesting case as a nice example of secretory carcinoma in an uncommon location. There are less than 50 cases reported in the thyroid. The morphology is similar to secretory carcinoma of the salivary gland and breast. Likewise, they demonstrate ETV6 locus rearrangement (ETV6-NTRK3 fusion). TRK inhibitors have been tried. Behavior is unpredictable with some reports suggesting frequent local recurrence risk while others report distant metastasis in up to 30% of cases.

References:

1. Chambers M, Nose V, Sadow PM, et al. Salivary-Like Tumors of the Thyroid: A Comprehensive Review of Three Rare Carcinomas. Head Neck Pathol 2021; 15:212-224.
2. Saliba M, Mohanty AS, Ho AL, et al. Secretory Carcinoma of the Thyroid in a 49-Year-Old Man Treated with Larotrectinib: Protracted Clinical Course of Disease Despite the High-Grade Histologic Features. Head Neck Pathol 2022 Jun;16(2):612-620.
3. Desai MA, Mehrad M, Ely KA et al. Secretory carcinoma of the thyroid gland: report of a highly aggressive case clinically mimicking undifferentiated carcinoma and review of the literature. Head Neck Pathol 2019; 13:562-572.

AMR SEMINAR #78
CASE 7

Contributed by: Ira Bleiweiss, M.D., University of Pennsylvania.

Clinical History: A 63 year old woman complained of a palpable mass in the axilla. Core biopsy yielded very scanty breast tissue with an atypical small glandular proliferation with a focus of perineural invasion, possibly representing low grade adenosquamous carcinoma (see below photos). It was felt to be insufficient for diagnosis and excision was recommended. The slides are from the excision.

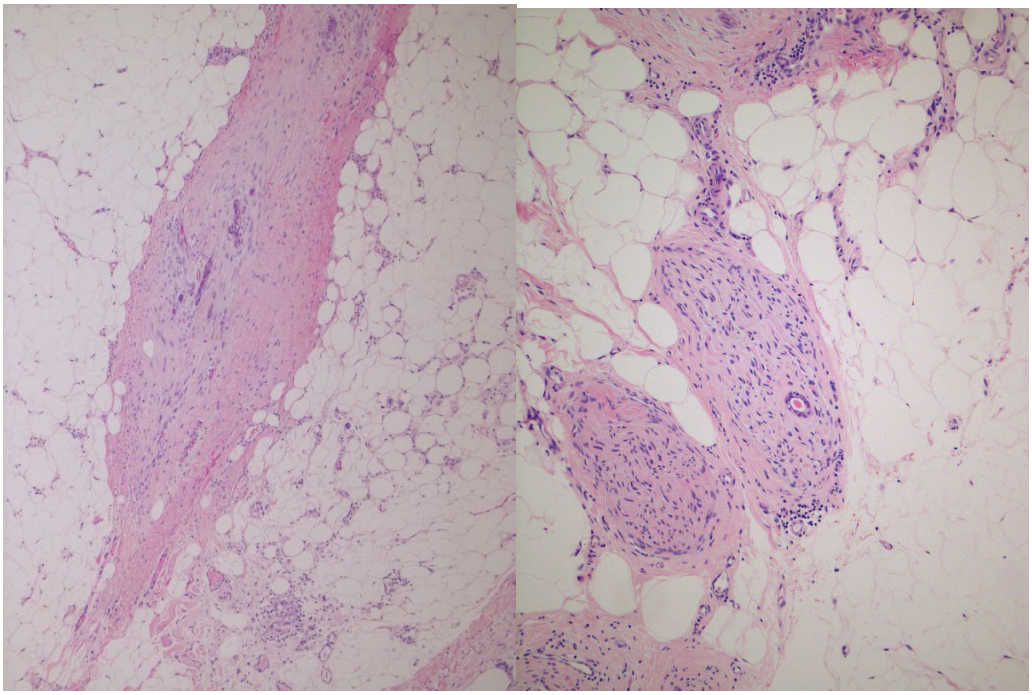

The excision followed soon thereafter, and the glass slides are from that specimen. With this appearance in mind, the surgeon was questioned more carefully and revealed that the mass was part of a longstanding "bump" in the skin which recently grew and caused the skin to be somewhat retracted. The bump was in the milk line. As you can see from the slides this is a well differentiated glandular process with squamous differentiation and keratinaceous cysts. The process surrounds normal breast ductal structures and does not appear to invade adipose tissue. The glands of this lesion have been described as akin to tadpoles as well as other interesting, imaginative appelations, and they seem to shrink with depth of the lesion. IHC for p63 show staining only of the outer (basal) layer of cells, not in the inner or squamous layer, oddly enough. In my (albeit limited) experience with low grade adenosquamous carcinoma, which is the main differential diagnosis for this lesion, all of the cells (i.e., both components of the tumor) are positive for p63.

Diagnosis: Syringomatous adenoma involving supernumerary nipple in the axilla.

AMR SEMINAR #78
CASE 8

Contributed by: John Gross, M.D., Johns Hopkins University.

Clinical History: A 62-year-old female with a past medical history significant for SLE, breast carcinoma (s/p chemoradiation, lumpectomy and axillary node dissection 18 years ago), cutaneous melanoma s/p wide excision 13 years ago, colonic adenocarcinoma s/p hemicolectomy and adjuvant chemotherapy 12 years ago and currently two years s/p resection of a spinal cord meningioma presents with an 8 cm esophageal mass involving all layers of her esophagus and abutting her aorta.

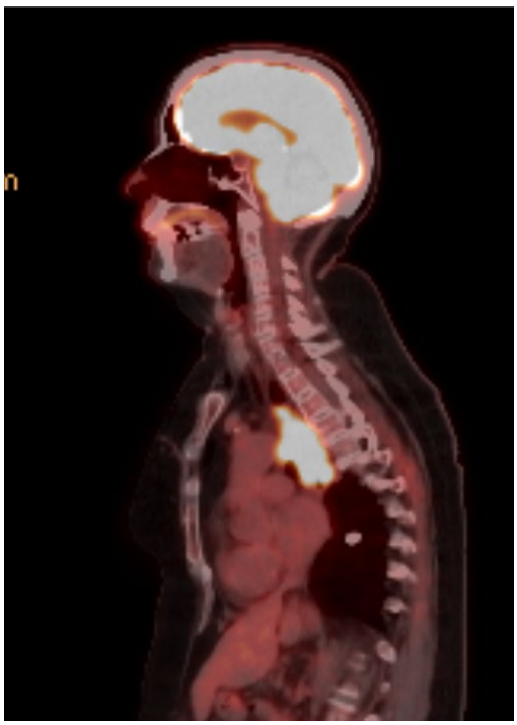

Sagittal PET Scan

Sagittal CT Scan

Pathologic Findings: Operative findings revealed a large tumor wrapping around the trachea posteriorly with extension into the left paratracheal nodes. Pathologic examination of the esophago-gastrectomy specimen revealed an aggressive 8.1 cm submucosal mass extending the entire thickness of the esophagus to the cauterized adventitial surfaces.

Histologic examination reveals a large ill-defined and infiltrative circumferential mass with an epicenter in the submucosa which extends through the peri-esophageal adventitial tissue to the radial (cauterized) margin. The tumor is composed of eosinophilic cells with round nuclei and variably eosinophilic cytoplasm. The cells of interest are relatively monotonous but various areas show unequivocal nuclear anaplasia and increased mitotic activity. In addition, and a helpful clue to the correct diagnosis is that the tumor assumes a perivascular pattern of growth best appreciated from low power. One of 26 lymph nodes was positive for metastatic tumor.

Immunohistochemistry was positive for SMA and collagen IV (special stain) whereas desmin, EMA, CK AE1/AE3, S100, BRAFV600E, Myogenin, and SOX10 were negative.

Sequencing identified a *MIR143::NOTCH2* (*CARMN(MIR143HG)::NOTCH2)* translocation. No *BRAF, NF1*, or *KRAS* mutations were detected.

Diagnosis: Malignant glomus tumor of esophagus.

Comment: Patient was discharged POD #10 but then was found to be in PEA / cardiac arrest at home (PD#12) with bright red hematemesis. Found to have an aorto-esophageal fistula. Resuscitations efforts unsuccessful and patient died (POD#12).

AMR SEMINAR #78
CASE 9

Contributed by: Maria Pia Foschini, M.D., University of Bologna, Italy.

Clinical History: A 61 year old man presented with an old standing ulcerated lesion involving the right cheek. The lesion had been present for a long time. In recent times, following the appearance of the ulcer, he delayed going to the hospital for fear of CoViD-19 infection.
CT scan evidenced a huge tumor, involving the right maxillary bone and half upper and lower lips on the same side. The tumor infiltrated the gingiva and cheek mucosa, reaching the overlying skin. After the diagnosis of minor salivary gland carcinoma, the patient underwent radical surgery with lymph-node dissection. No lymph-nodes metastases were detected (45 lymph-nodes examined). No distant metastases were detected at the time of the surgery.
Six months after surgery, a lung nodule appeared. A transthoracic biopsy confirmed the metastatic origin and the nodule was surgically resected. The patient is presently alive, in follow-up, without any further evidence of disease (1 year after primary surgery).

Pathologic Findings: The surgical specimen consisted of the right side of the face, including the right cheek, right half of the upper and lower lips, and the base of the nose. Moreover, there was a portion of maxillary bone, with two incisor and maxillary sinus. The right-side cervical dissection contained 45 lymph-nodes. The tumor had a major axis of 6 cm, involved the whole thickness of the cheek ulcerating both the skin and the mucosa. The tumor was composed of nests of small, quite uniform, neoplastic cells, with scant cytoplasm and inconspicuous nucleoli. Nests were mainly solid, with some focal small glandular spaces reminiscent of a cribriform architecture. A wide central area of necrosis was seen. Perineural and endovascular invasion were seen. By immunohistochemistry the neoplastic cells were positive for CK7, p63, SOX10, p16 and Bcl2. S100, CK14, p40 and smooth muscle actin were negative. CD117 was focally positive. The Ki-67 labelling index was up to 20%; p53 was not overexpressed. CK7 was mainly positive in the central part of the neoplastic nests, while p63 was positive at the periphery. We did not have the possibility to test for PRKD.

Diagnosis: Polymorphous adenocarcinoma of minor salivary gland with features of high-grade transformation.

Comment: The present case had an unusual growth pattern and immunohistochemical profile. Differential diagnoses included epithelial-myoepithelial carcinoma (EMCC), adenoid-cystic carcinoma (AdCC) and polymorphous adenocarcinoma (PAC).

The CK7 and p63 distribution pattern was reminiscent of EMCC, but the H&E appearance characterized by uniform cells, negativity for other myoepithelial cell markers contrasted with this diagnosis. Similarly, AdCC was excluded as the tumor lacked the cribriform pattern with the typical dual type of mucins. In addition, CD117 showed focal positivity only.
Therefore, the PAC diagnosis, based on morphology and immunohistochemical profile, seemed the most probable, even if S100 negativity is not typical of PAC.

Polymorphous Adenocarcinoma (PAC) of the salivary glands is a rare cancer with an incidence of 0.051 cases per 100 000 individuals and it is characterized by cytological uniformity and morphological diversity. PAC has an excellent prognosis, with local recurrence rates of 10-33% and rare distant metastases reported. Papillary and cribriform pattern are independent adverse prognostic factors. Despite average presentation, PAC can demonstrate a "high grade" behavior, infiltrating adjacent structures and ulcerating the skin. Even if cases of regional and distant metastasis have been described, this tumor is still considered as a low risk histology lesion. According to the WHO blue book, published in 2017, PAC comprises different variants, based on architectural patterns.

Specifically, PAC cribriform variant, include the "Cribriform Adenocarcinoma of the tongue" (CAT). CAT was first described by Michal and colleagues in 1999. At the time, the neoplastic peculiarities described were a propensity to the posterior tongue, a lobulated architecture, a predominant solid structure, microcystic and cribriform grow pattern, and a uniform type of tumor cells, with ground-glass optically cleared nuclei. Subsequent studies demonstrated this tumor occurs also in other areas of the oral cavity. A revised terminology suggested "Cribriform Adenocarcinoma of Salivary Glands" (CASG) that remains a controversial entity, with differences from PAC and worse prognosis.

The present case had an unusual profile, not completely typical but reminiscent of PAC. In addition, the solid nests, presence of extensive necrosis, high mitotic count, extensive perineural invasion, are suggestive of high grade transformation. Nevertheless, despite all these features, and of the clinical history of long standing lesion, no lymph-node metastases were present at the time of surgery. One lung metastasis appeared 6 months later, was surgically treated and the patient at last follow-up (December 2021) did not show evidence of disease.
I am happy to hear your opinion!

References:

- Rooper LM. Challenges in Minor Salivary Gland Biopsies: A Practical Approach to Problematic Histologic Patterns. Head Neck Pathol. 2019 Sep;13(3):476-484. doi: 10.1007/s12105-019-01010-8. Epub 2019 Mar 18. PMID: 30887392; PMCID: PMC6684710.
- Hernandez-Prera JC. Historical Evolution of the Polymorphous Adenocarcinoma. Head Neck Pathol. 2019 Sep;13(3):415-422. doi: 10.1007/s12105-018-0964-9. Epub 2018 Sep 5. PMID: 30187348; PMCID: PMC6684715.
- Vander Poorten V, Triantafyllou A, Skálová A, Stenman G, Bishop JA, Hauben E, Hunt JL, Hellquist H, Feys S, De Bree R, Mäkitie AA, Quer M, Strojan P, Guntinas-Lichius O, Rinaldo A, Ferlito A. Polymorphous adenocarcinoma of the salivary glands: reappraisal and update. Eur Arch Otorhinolaryngol. 2018 Jul;275(7):1681-1695. doi: 10.1007/s00405-018-4985-5. Epub 2018 May 14. PMID: 29761209.

- Michal M, Skálová A, Simpson RH, Raslan WF, Curík R, Leivo I, Mukensnábl P. Cribriform adenocarcinoma of the tongue: a hitherto unrecognized type of adenocarcinoma characteristically occurring in the tongue. Histopathology. 1999 Dec;35(6):495-501. doi: 10.1046/j.1365-2559.1999.00792.x. PMID: 10583573.
- Kikuchi K, Nagao T, Ide F, Takizawa S, Sakashita H, Tsujino I, Li TJ, Kusama K. Palatal Polymorphous Adenocarcinoma with High-Grade Transformation: A Case Report and Literature Review. Head Neck Pathol. 2019 Jun;13(2):131-139. doi: 10.1007/s12105-018-0916-4. Epub 2018 Mar 29. PMID: 29594833; PMCID: PMC6513909.

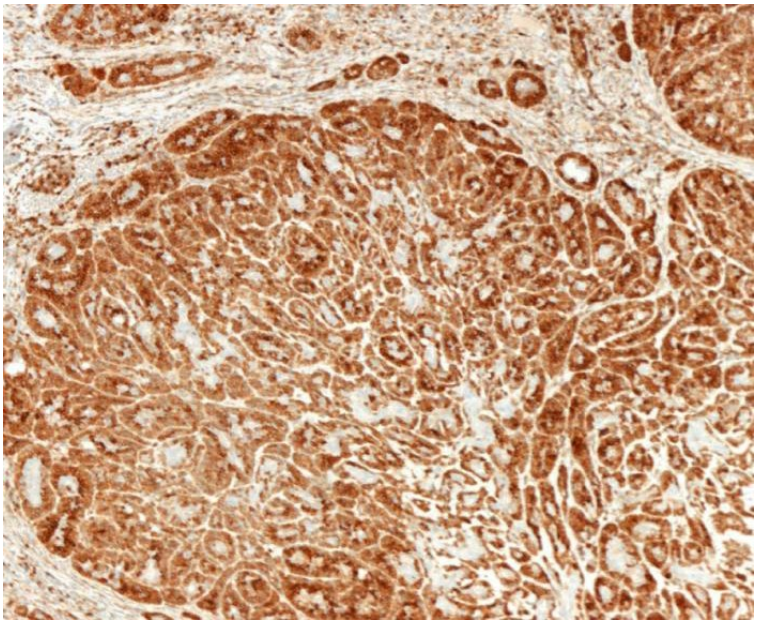

BCL-2

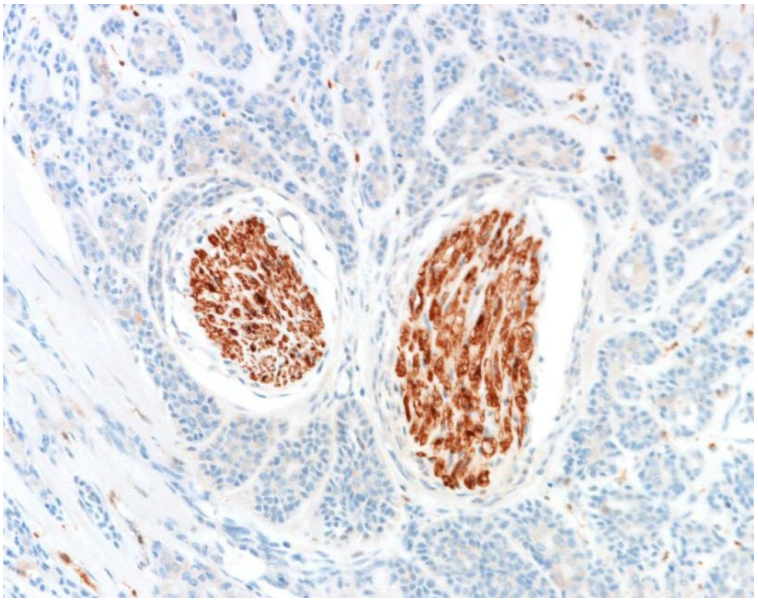

S100

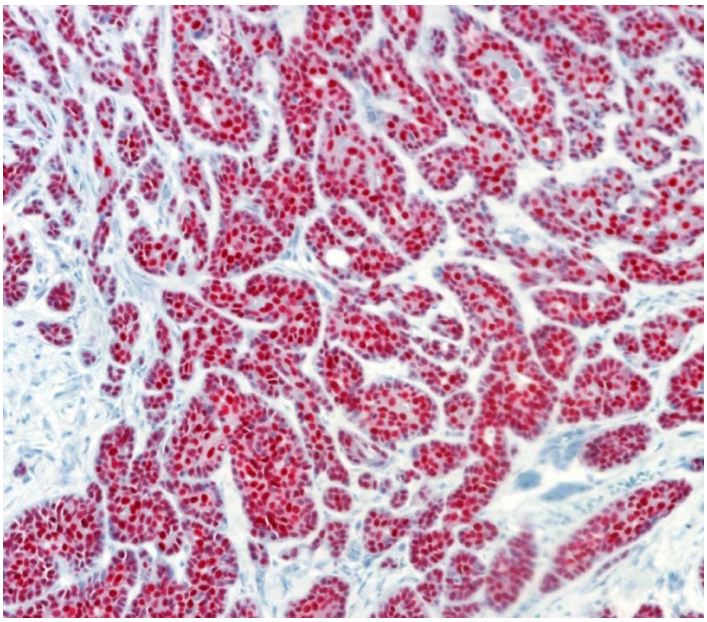

SOX10

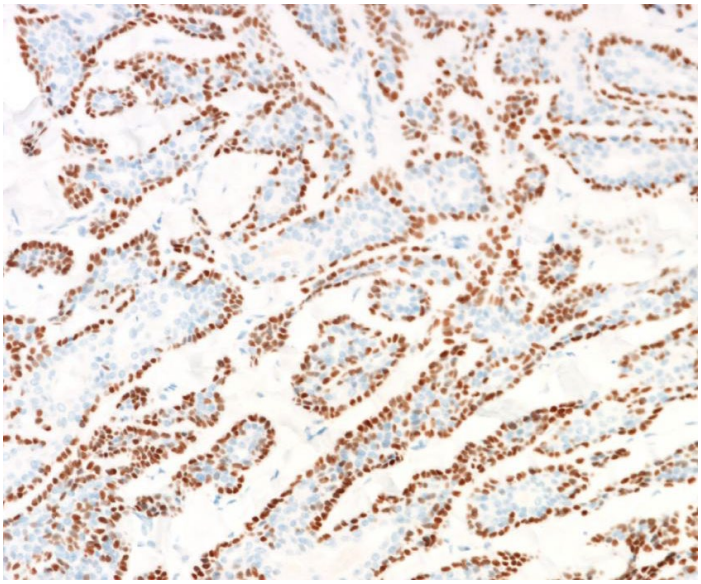

p63

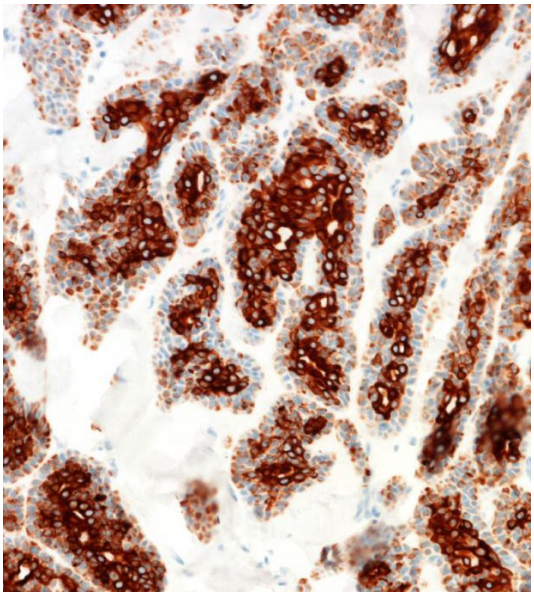

CK7

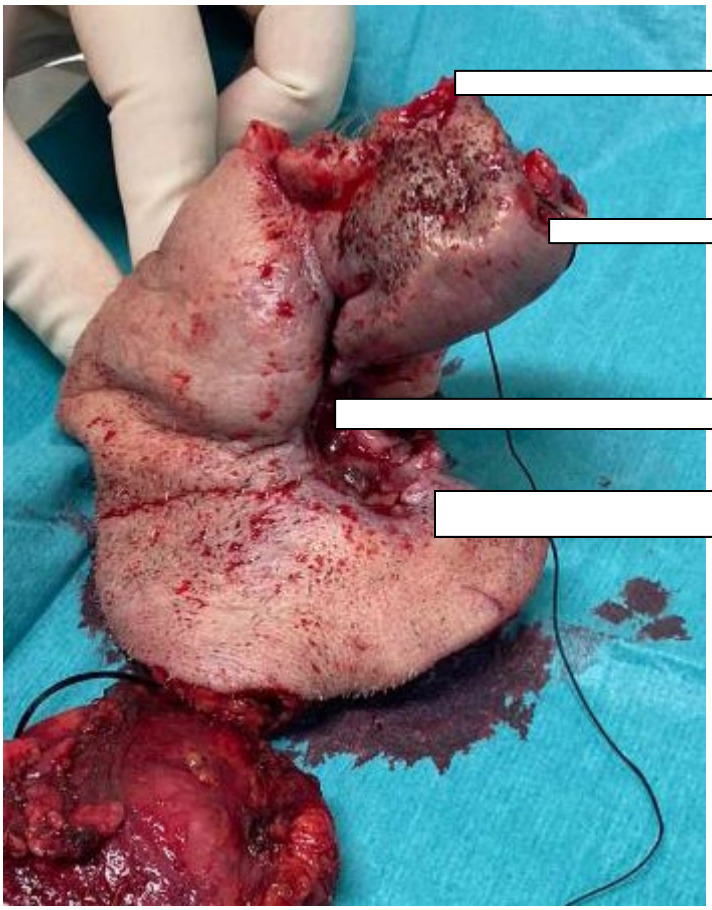

Base of nose

Upper lip

Ulcer

Lower lip

AMR SEMINAR #78
CASE 10

Contributed by: Paul Wakely, Jr., M.D., Ohio State University.

History: A 41 year-old woman presented with a right buttock mass of unknown duration. She has no other lesions. Core needle biopsy showed a low -grade spindle cell lesion diagnosed as possible solitary fibrous tumor or DFSP. A wide resection was then performed from which you have slides.

Pathologic Findings: A 4.7 cm. lobulated tan-white solid mass was removed with clear margins. Low-power examination shows a diffuse mixed inflammatory cell and foamy histiocytic cell infiltrate having a high percentage of eosinophils, and a vaguely fascicular spindle cell proliferation. Closer examination highlights the atypical cytologic features of: nuclear enlargement, nuclear pleomorphism, coarse irregularly dispersed chromatin, and enlarged nucleoli. Some pleomorphic cells display striking macronucleoli imitating so-called inclusion-type nucleoli. Focal hemosiderin deposition is present. Mitotic activity however is almost non-existent. IHC stains showed diffuse vimentin and CD34 expression with negative staining for CD31, CD30, EBV, S-100, Alk-1, CD1a, EMA, and actin.

Diagnosis: Myxoinflammatory Fibroblastic Sarcoma [MiFS].

Comment: This case is many years old, so no molecular testing was available at that time. To my knowledge, no recurrence or metastasis has occurred in this patient in almost 15 years since resection. Because of its non-acral location, and the absence of appreciable myxoid stroma, it was debated at the time whether this was truly an example of MiFS, or just an atypical form of inflammatory myofibroblastic tumor. As you note, staining was also performed to exclude a Langerhans type histiocytosis. We finally 'settled' on a diagnosis of MiFS, but I am still not completely convinced because MiFS lacks a characteristic immunohistochemical signature, and a diagnostic molecular abnormality. Opinions from members of the club are most welcome.

Selected References:

• Lucas DR. Myxoinflammatory Fibroblastic Sarcoma: review and update. Arch Pathol Lab Med. 2017 Nov;141(11):1503-1507.

• Boland JM, Folpe AL. Hemosiderotic Fibrolipomatous Tumor, Pleomorphic Hyalinizing Angiectatic Tumor, and Myxoinflammatory Fibroblastic Sarcoma: related or not? Adv Anat Pathol. 2017;24:268-277.

• Wangsiricharoen S, Ali SZ, Wakely PE Jr. Cytopathology of myxoinflammatory fibroblastic sarcoma: a series of eight cases and review of the literature. J Am Soc Cytopathol. 2021;10:310-320.

AMR SEMINAR #78
CASE 11

Contributed by: Reza Alaghehbandan, M.D., Cleveland Clinic.

Case History: A 32-year-old woman presented with hydronephrosis. Imaging revealed 8.5 cm renal mass in the left kidney.

Gross findings: A well-circumscribed brown-mahogany solid mass with areas of hemorrhage and necrosis measuring 8.5 x 7.3 x 7 cm, located in the upper and middle poles of the kidney. The tumor invades into the renal sinus fat but not perinephric adipose tissue.

Microscopic findings: The tumor is well-circumscribed, but non-encapsulated, and composed of very uniform population of oncocytic cells with round-to-oval nuclei and generally without perinuclear clearing. Although the neoplastic cells generally have diffuse and compact nested growth, there are very limited foci with tubular, papillary, cystic, and reticular growth patterns. Further, there are foci demonstrating slightly enlarged nuclei with more prominent nucleoli, but no significant cell atypia. Focally, there is a mucinous background, as well as focal luminal content in the tubules. Rare mitotic figures are present. There are quite distinct areas of tumor necrosis. There are also distinct areas of fresh hemorrhage and fibrin deposition along with foci of scattered foamy macrophages and lymphocytic aggregates.

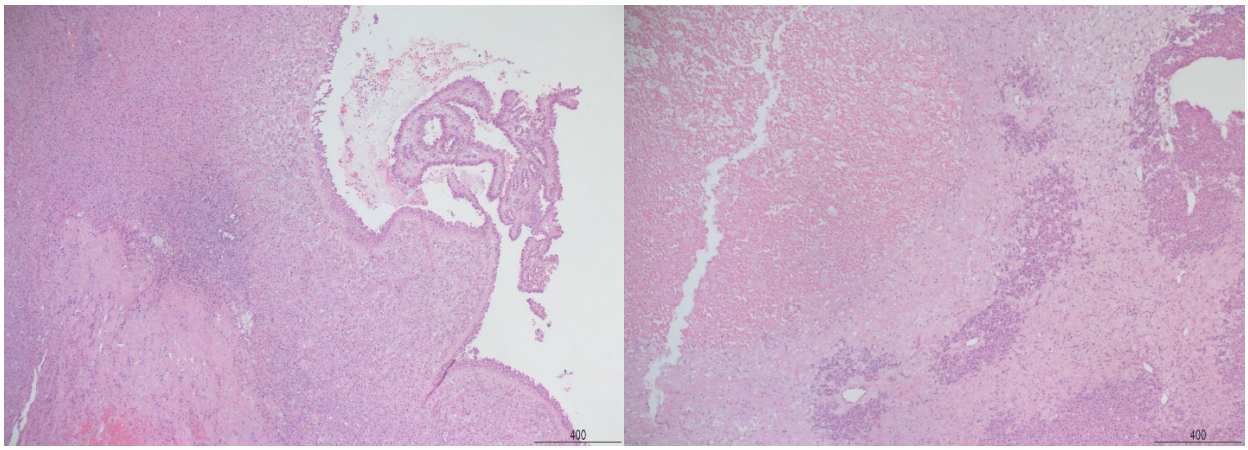

Immunohistochemically, the neoplastic cells were negative for CD117, while only rare cells were positive for CK7. FH and SDH were both retained. Other positive stains included PAX8, GATA3, AMACR (focal), vimentin (focal), and CD10 (focal). Cathepsin K, Alk1, CK5/6, HMB45 and melan A were completely negative.

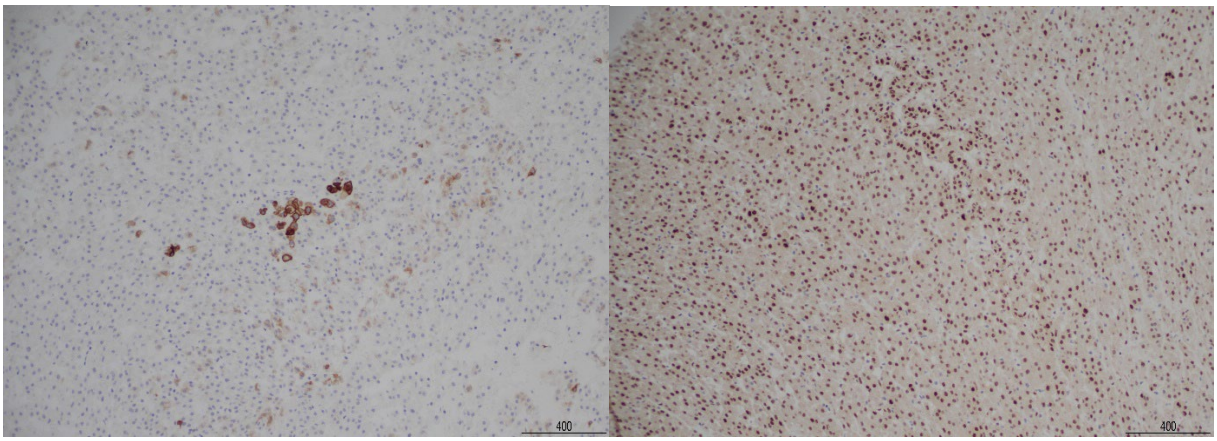

CK7 **GATA3**

Diagnosis: Renal cell carcinoma with oncocytic features, unclassified.

Comments: In summary, this tumor falls into the category of renal oncocytic neoplasms. This field of uropathology has undergone a renaissance in the last decade with new and novel entities being described (e.g., LOT, EVT). This tumor is peculiar although it does have some morphologic similarities with LOT (low-grade oncocytic tumor), but it does not fulfill its morphologic and immunohistochemical criteria. It certainly does not fall into renal oncocytoma or chromophobe RCC (ChRCC) either. The presence of mucin, necrosis, and variable morphologic growth patterns are also unusual features. Some may consider such tumor as an "oncocytic renal neoplasm, not further specified". However, given the presence of worrisome histologic features such as sinus fat invasion and tumor necrosis, I believe it is best classified as an RCC with oncocytic features. In Fact, the most recent 2022 WHO Classification of Renal tumors include renal oncocytoma, ChRCC and Unclassified RCC as low grade oncocytic tumors. Such tumors in our experience tend to behave in more favourable fashion with rare lymph node and/or distance metastasis.

Given the young age of the patient and the large size of the tumor (8.5 cm), I also suggested to perform a clinical correlation for possible genetic/hereditary underlying condition, such as tubular sclerosis (TSC), as well as to perform additional molecular studies to evaluate for possible genetic abnormalities (i.e., TSC/mTOR pathway mutations).

Selected references

- Amin MB, McKenney JK, Martignoni G, Campbell SC, Pal S, Tickoo SK. Low grade oncocytic tumors of the kidney: a clinically relevant approach for the workup and accurate diagnosis. Mod Pathol. 2022 Jul 27. doi: 10.1038/s41379-022-01108-5. Epub ahead of print. PMID: 35896615.
- Hes O, Trpkov K. Do we need an updated classification of oncocytic renal tumors? Emergence of low-grade oncocytic tumor (LOT) and eosinophilic vacuolated tumor (EVT) as novel renal entities. Mod Pathol. 2022 Mar 10. doi: 10.1038/s41379-022-01057-z. Epub ahead of print. PMID: 35273336.
- Trpkov K, Williamson SR, Gill AJ, Adeniran AJ, Agaimy A, Alaghehbandan R, Amin MB, Argani P, Chen YB, Cheng L, Epstein JI, Cheville JC, Comperat E, da Cunha IW,

Gordetsky JB, Gupta S, He H, Hirsch MS, Humphrey PA, Kapur P, Kojima F, Lopez JI, Maclean F, Magi-Galluzzi C, McKenney JK, Mehra R, Menon S, Netto GJ, Przybycin CG, Rao P, Rao Q, Reuter VE, Saleeb RM, Shah RB, Smith SC, Tickoo S, Tretiakova MS, True L, Verkarre V, Wobker SE, Zhou M, Hes O. Novel, emerging and provisional renal entities: The Genitourinary Pathology Society (GUPS) update on renal neoplasia. Mod Pathol. 2021 Jun;34(6):1167-1184.

AMR SEMINAR #78
CASE 12

Contributed by: Ricardo Lastra, M.D., University of Chicago.

Clinical History: A 52 year-old female without significant personal medical history presented with nonspecific abdominopelvic pain. Imaging studies revealed a 3.1 cm mass in the upper pole of the right kidney, as well as a 2.3 cm solid right ovarian mass. She underwent right partial nephrectomy and right salpingo-oophorectomy with frozen section evaluation. Upon final evaluation of permanent sections, the renal mass was consistent with a mixed epithelial and stromal tumor (MEST).

Microscopic Sections: Histologic evaluation of the right ovarian mass demonstrated an expansile, variably cystic proliferation of papillary and tubulocystic structures with slender and delicate fibrovascular cores. The papillae are lined by a single layer of bland cuboidal to columnar cells with sharply delineated cell borders, demonstrating variably clear to eosinophilic cytoplasm. The nuclei are round with uniform chromatin pattern and inconspicuous nucleoli. In some areas, the nuclei were polarized in series towards either the luminal or basal surfaces, focally resembling secretory endometrium. No significant cytologic atypia, necrosis, or mitotic activity was appreciable, and areas of infiltrative/destructive growth were not present.

Immunohistochemical and Molecular Findings: Immunohistochemical stains demonstrate the lesional cells to be diffusely positive for EMA, CK7, MOC-31, BerEp4, PAX-8, WT-1, D2-40, CK5/6, HBME-1, calretinin, and CA-IX ('cup-shaped' positivity with basolateral membrane staining, but absence of apical staining). In addition, the lesional cells were negative for claudin-4, inhibin, CD10, RCC, AMACR/P504s, ER, and PR. Lastly, BAP-1 demonstrated retained nuclear expression.
Next generation sequencing demonstrated the presence of a pathogenic mutation in the VHL gene (VHL c.343C>T, p.H115Y) with low allele frequency (7%).

Diagnosis: Ovarian clear cell papillary cystadenoma (CCPA).

Comments: Clear cell papillary cystadenoma of the epididymis is a well-described entity, recognized as one of the benign manifestations of von Hippel-Lindau disease (VHLD). Historically, these preceded the description of a histologically similar lesion in the female genital tract, most commonly localized to the broad ligament.[1-4] Only one of the few documented cases in the female genital tract has exhibited aggressive behavior, with peritoneal spread in a patient without VHLD.[5] Thus far, there is no consensus regarding the true lineage of these lesions – whether they are of mesonephric, M*ü*llerian, or even mesothelial origin.

An apparently low-grade, unilateral ovarian tumor with predominantly papillary and tubulocystic architecture, and cytoplasmic clearing were features initially leading to an intraoperative misdiagnosis of metastatic CCRCC. Even on permanent evaluation, this was a strong primary

contender given the cytoplasmic features and the patient's concurrent renal tumor. However, the alveolar architecture, arborizing vasculature, and prominent nucleoli characteristic of a metastatic CCRCC were lacking. Strong CK7 expression essentially also dismissed the diagnosis of CCRCC.

Given the location, PAX-8 positivity, and some evidence of epithelial differentiation, primary epithelial lesions of the ovary were also entertained. Most typical histomorphologic features of clear cell M*ü*llerian lesions were lacking. Characteristic immunophenotypic (WT-1 negative, Napsin-A positive) and architectural features (prominent nuclear atypia and destructive invasion) of an ovarian clear cell carcinoma were not present

While clear cell cytology is rarely encountered in mesothelial proliferations, entities along this spectrum were considered. These tumors, ranging from well-differentiated papillary to malignant mesotheliomas, usually arise from peritoneal surfaces. While there was no ovarian surface involvement by the tumor here, the architectural features – namely, peripheral displacement of native ovarian structures – lend support to the hypothesis that it likely arose from mesothelial lining at the hilum and pushed, rather than infiltrated, inwards. Indeed, despite its name, CCPA might well be of partial mesothelial divergence given its immunohistochemical profile as outlined here and in the literature. Most typical mesothelial markers were focally to diffusely positive (WT-1, calretinin, D2-40, and HBME1). However, the immunoreactivity of those specifically employed to differentiate mesothelial from epithelial lineage (MOC-31 and BerEp4) was too strong for a solely mesothelial proliferation. Positivity for PAX-8 was additionally misleading; however, this is documented as an exceptional feature of both benign and malignant mesothelial tumors.[6]

Conclusive evidence was obtained via NGS, which revealed a point mutation in the VHL coding region of exon 2. This particular variant, which results in an aberrant histidine to tyrosine substitution at amino acid 115 of the von Hippel-Lindau tumor suppressor protein, is a known 'hotspot' mutation site. It has been documented in papillary cystadenomas of both males and females, in clear cell renal cell carcinomas, and a peritoneal mesothelioma with clear cell features.[7] The patient had no known associations with VHLD upon follow-up, and the low variant allele frequency found on mutational analysis corroborated the likely sporadic nature of this case.

A majority of reported CCPA were associated with VHLD, in which they were incidentally detected during workup of another pathology. They typically occurred in patients between the ages of 20 and 60, and – in contrast to their epididymal counterpart – were unilateral even in the context of VHLD. Immunohistochemically, they were consistently positive for low-molecular weight cytokeratin, EMA, BerEp4, CK7, CD10, and vimentin. They were variably positive for mesothelial markers (calretinin, HBME-1, WT-1), and consistently negative for ER and PR. They characteristically display a 'cup-like' pattern of staining with CA-IX, with presence of basolatareal staining but absence of staining at the apical portion of the cells. All were centered in the mesosalpinx or elsewhere in the broad ligament, save one which was embedded within the muscular wall of the fallopian tube without intraluminal extension.[5] Based on the follow-up available from these reports, local excision is evidently curative. While there are no instances of recurrence, one paper has described regional spread from a primary mesosalpingeal location to

the ipsilateral ovary and omentum.[3] These were determined to be 'benign implants' with similar immunophenotype as the mesosalpingeal primary.

References:

1. Cox R, Vang R, Epstein JI. Papillary cystadenoma of the epididymis and broad ligament: morphologic and immunohistochemical overlap with clear cell papillary renal cell carcinoma. Am J Surg Pathol. 2014;38(5):713-718.
2. Gersell DJ, King TC. Papillary cystadenoma of the mesosalpinx in von Hippel-Lindau disease. Am J Surg Pathol. 1988;12(2):145-149.
3. Nogales FF, Goyenaga P, Preda O, et al. An analysis of five clear cell papillary cystadenomas of mesosalpinx and broad ligament: four associated with von Hippel-Lindau disease and one aggressive sporadic type. Histopathology. 2012;60(5):748-757.
4. Shen T, Zhuang Z, Gersell DJ, Tavassoli FA. Allelic Deletion of VHL Gene Detected in Papillary Tumors of the Broad Ligament, Epididymis, and Retroperitoneum in von Hippel-Lindau Disease Patients. Int J Surg Pathol. 2000;8(3):207-212.
5. Gaffey MJ, Mills SE, Boyd JC. Aggressive papillary tumor of middle ear/temporal bone and adnexal papillary cystadenoma. Manifestations of von Hippel-Lindau disease. Am J Surg Pathol. 1994;18(12):1254-1260.
6. Chapel DB, Husain AN, Krausz T, McGregor SM. PAX8 Expression in a Subset of Malignant Peritoneal Mesotheliomas and Benign Mesothelium has Diagnostic Implications in the Differential Diagnosis of Ovarian Serous Carcinoma. Am J Surg Pathol. 2017;41(12):1675-1682.
7. Smith-Hannah A, Naous R. Primary peritoneal epithelioid mesothelioma of clear cell type with a novel VHL gene mutation: a case report. Hum Pathol. 2019;83:199-203.

AMR SEMINAR #78
CASE 13

Contributed by: Thomas Mentzel, M.D., Germany.

Clinical History: A 6-weeks-old female patient presented with a large, pigmented lesion at the back of her head, and a congenital naevus was suspected. However, the centre of the lesion was indurated, and MRI-scans revealed a destruction of the underlying bone. A large biopsy has been performed.

Pathological Findings: A band-like proliferation of slightly enlarged, round to epithelioid, pigmented melanocytic cells is seen in upper parts of the dermis. Below a fibrosis with inflammation, numerous dilated vessels, spindled cells and more cellular nests and bundles is noted. A proliferation of bland spindle-shaped cells infiltrating the bone is evident in lower parts of the biopsy. Immunohistochemically, the melanocytic cells stain positively for S-100 protein, Sox10, Melan-A and HMB-45. S-100 protein staining reveal in addition a network of bland spindled cells (that are negative for Sox10), and the cellular bundles and nests are composed of S-100 and CD34-positive spindle-shaped cells. The infiltrating spindled cells in lower parts of the biopsy stain homogeneously positive for CD34. The endothelial cells of numerous associated vessels show loss of WT-1 expression. Additional molecular studies did not show mutations of the *BRAF, NRAS*, *GNAQ* or *GNA11* genes.

Diagnosis: Cutaneous neurocristic hamartoma (with prominent malformative vessels)

Comments: Cutaneous neurocristic hamartoma represents a rare entity resulting from aberrant development of the neuromesenchyme. These lesions may reach a considerable size and may destroy underlying bone or infiltrate bone marrow. Neurocristic hamartomas are composed of nevomelanocytes, Schwann cells, neurosustentacular cells, neuromesenchymal and fibroblastic cells. In some cases, additional elements as cartilage, bone, and numerous vessels (as in our case) are present, and dermal hyperneury has been reported. These hamartomas are usually present at birth but may develop in childhood and adolescents as well. Of note there is a high incidence of malignant transformation and the development of a malignant melanoma. These malignant lesions are designated as cutaneous malignant melanotic neurocristic tumours.

References:

- Bevona C et al. Dermal melanocytic proliferation with features of a plaque-type blue nevus and neurocristic hamartoma. J Am Acad Dermatol 2003; 49: 924-929
- Conrad DM et al. Extensive neurocristic hamartoma with bone marrow involvement. Am J Dermatopathol 2010; 32: 486-488
- Karamitopoulou-Diamantis E et al. Cutaneous neurocristic hamartoma with blue nevus-like features and plexiform dermal hyperneury. Histopathology 2006; 49: 326-328
- Mezebish D et al. Neurocristic cutaneous hamartoma: a distinctive dermal melanocytosis with an unknown malignant potential. Mod Pathol 1998; 11: 573-578

- Pathy AL et al. Malignant melanoma arising in a blue nevus with features of pilar neurocristic hamartoma. J Cutan Pathol 1993; 20: 459-464
- Pearson JP et al. Cutaneous malignant neurocristic tumors arising in neurocristic hamartomas. A melanocytic tumor morphologically and biologically distinct from common melanoma. Am J Surg Pathol 1996; 20: 665-677
- Smith KJ et al. The spectrum of neurocristic cutaneous hamartoma: clinicopathologic and immunohistochemical study of three cases. Ann Diagn Pathol 1998; 2: 213-223
- Stieler KM et al. Cutaneous cephalic neurocristic hamartoma on the head with melanocytic, cartilage, blood vessel, neural, and bony tissue. Am J Dermatopathol 2021; 43: 284-286

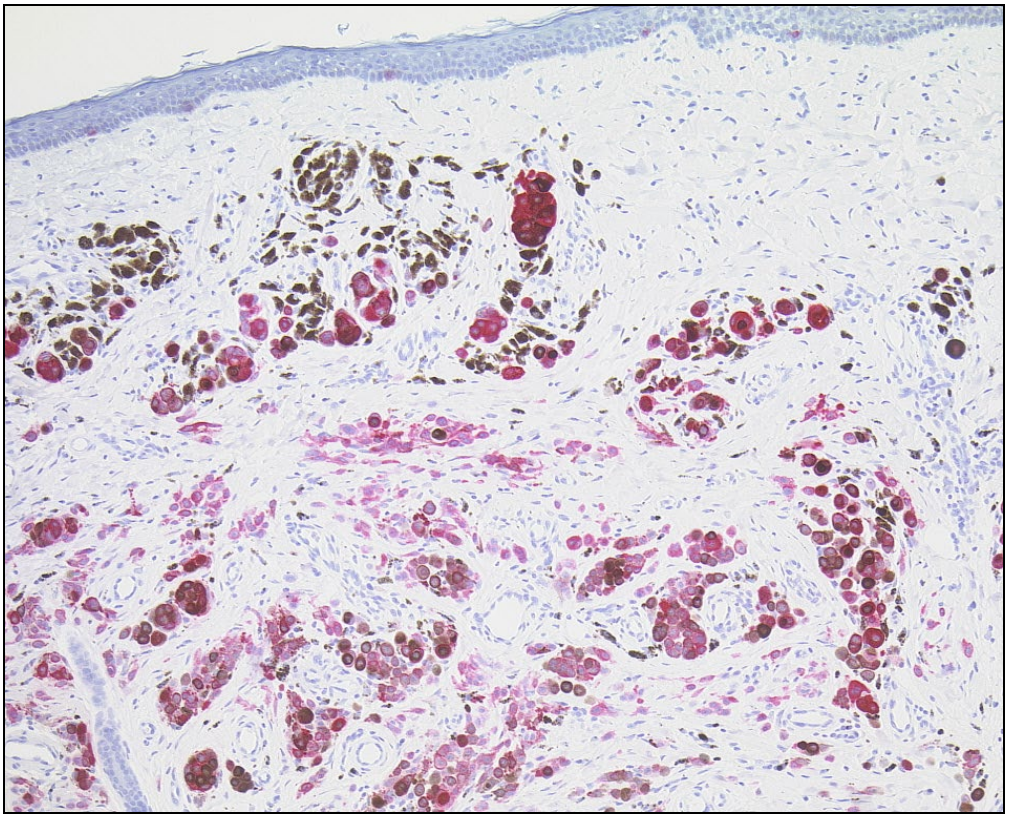

HMB-45

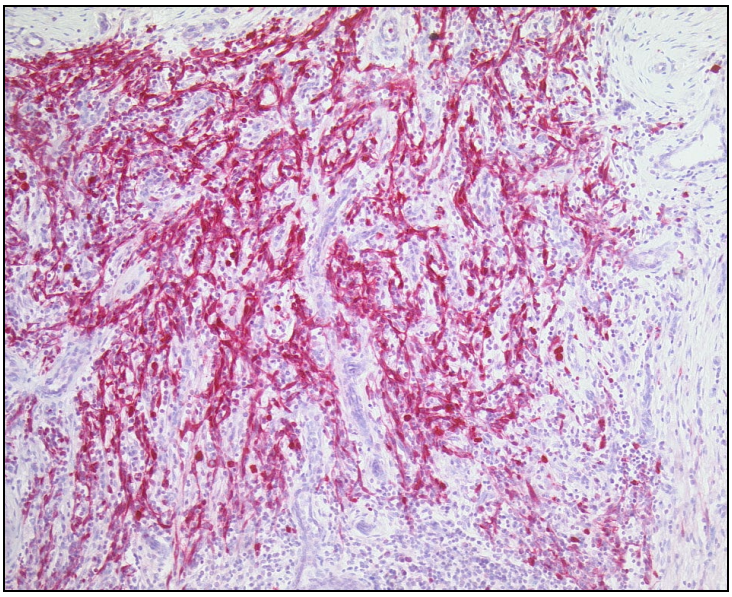

S-100 protein

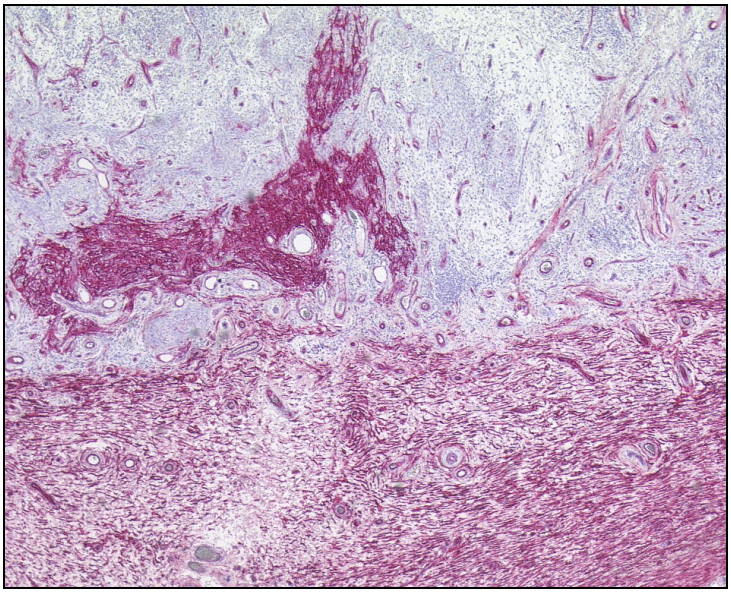

CD34 (HPCA-1)

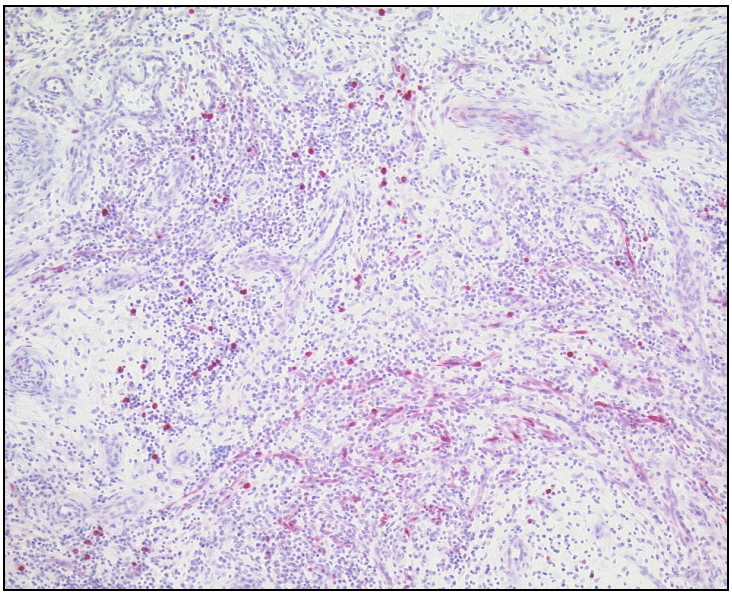

WT-1

AMR SEMINAR #78
CASE 14

Contributed by: Goran Elmberger, M.D., Linkoping University Hospital, Sweden.

Clinical History: A 60-year-old woman with persistent cough, ex-smoker, with history of 30 pack-years. Father died from lung cancer at 65 years age. X-ray/CT/PET initially interpreted as atelectasis. Unresolved at control. A 25 mm partly solid infiltrate peripherally in right lower lobe was seen. CT guided core biopsy was performed including molecular analysis and then a surgical resection was performed.

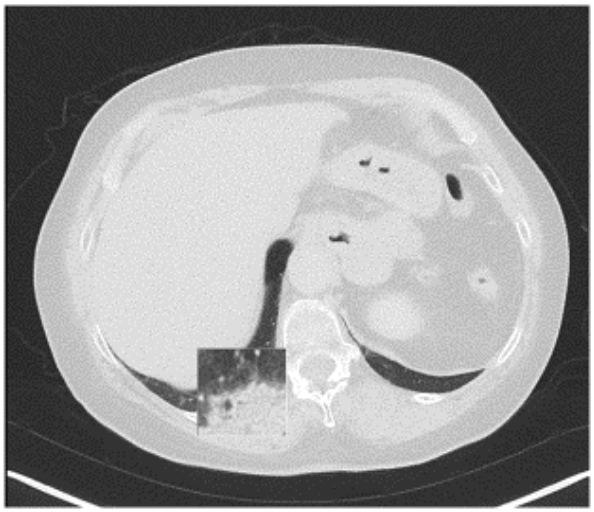

Pathological Findings: Microscopy show a subpleural well differentiated mucinous adenocarcinoma with a lepidic/STAS component and a more solid area with inflamed stroma and partial loss of elastin fibers between crowded acinar glandular formations. Tumor cells show a columnar cell morphology with abundant intracytoplasmic mucin and small, basally oriented nuclei. Nuclear atypia is inconspicuous. Lots of intraalveolar mucin surround the tumor. Largest microscopical dimension including solid and lepidic components is 18 mm. Size of the solid component is 10 mm. The surrounding lung parenchyma is essentially normal with only some anthracotic pigmentation. Radically excised. No pleural invasion. No lymphovascular growth. Intralobar and other mediastinal sampled lymph node stations without metastases.

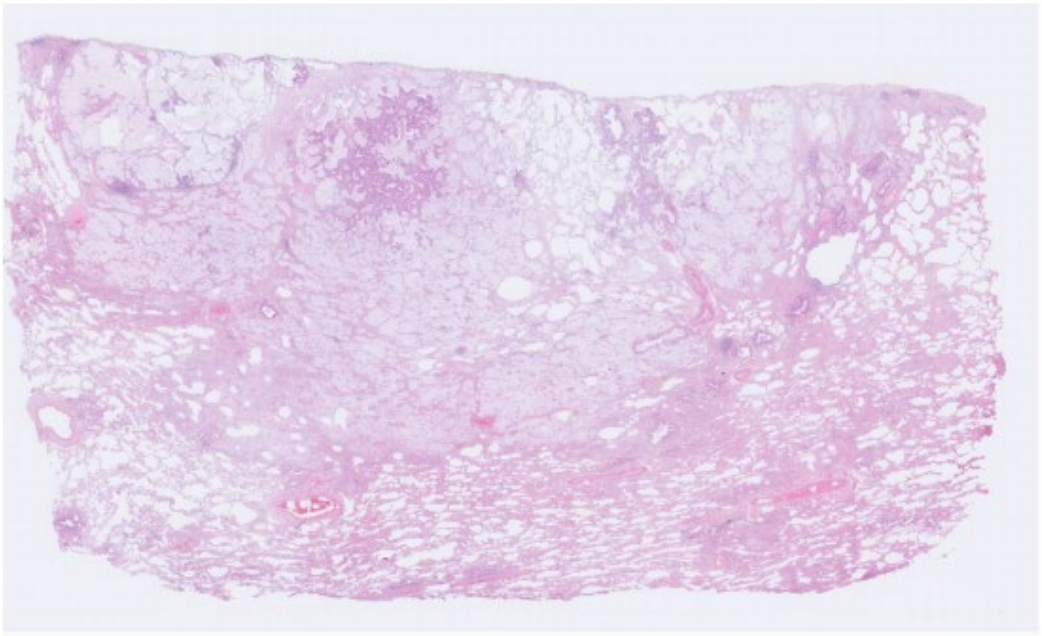

Immunohistochemistry*:* showed CKAE1/AE3+, CK7+, CK20 -/+, CDX2-, TTF1 -phenotype.

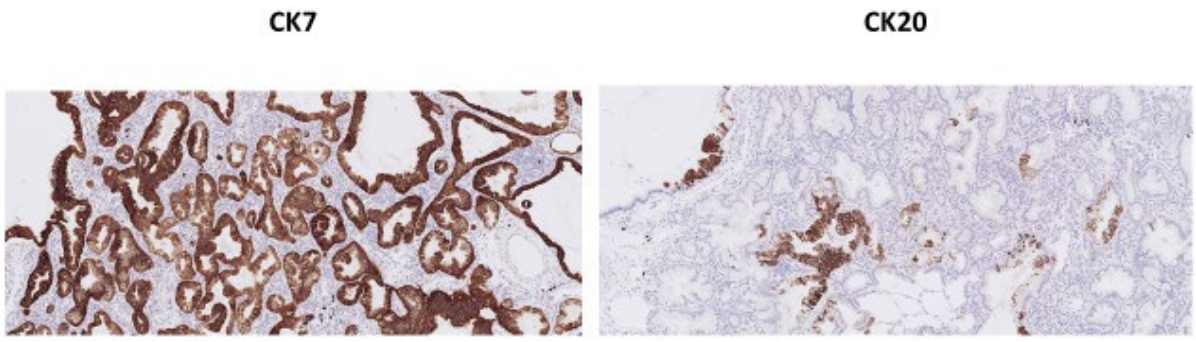

Molecular testing revealed a rather unusual and recently described translocation with gene fusion *CD74-NRG1*.

Diagnosis: Pulmonary invasive mucinous adenocarcinoma (IMA) with CD74-NRG1 fusion.

Follow-up: Radical excision of carcinoma pT1bN0. Clinical and radiological examination did not find systemic metastases or other primary tumor. Uneventful follow-up now only at 3 months.

Discussion: Adenocarcinoma in situ, minimally invasive adenocarcinoma, lepidic predominant adenocarcinoma and invasive mucinous adenocarcinoma are relatively new classification entities which replace the now retired term, bronchioloalveolar carcinoma (BAC). A thorough understanding of the new classification is essential for pathologists to provide accurate diagnosis, staging and a molecular basis for treatment.

Definition and history: Invasive mucinous adenocarcinoma (IMA) was introduced in the WHO classification 2015 4th edition and largely replaced the former mucinous bronchioloalveolar carcinoma category. IMAs are less prevalent than are invasive non-mucinous adenocarcinomas (INMAs), accounting for approximately 5% of lung adenocarcinomas. The rationale for separation of invasive mucinous adenocarcinoma from nonmucinous adenocarcinomas was that multiple studies indicated that IMA's had major clinical, radiologic, pathologic, and genetic differences from the tumors formerly classified as nonmucinous BAC. In particular, these tumors showed a very strong correlation with KRAS mutations whereas nonmucinous adenocarcinomas were more likely to show EGFR mutation and only occasionally KRAS mutation. The neoplasms formerly termed mucinous BAC's were recognized to have invasive components in the majority of cases, and were thus reclassified as invasive mucinous adenocarcinomas.

Imaging: The CT appearance of these lesions varies wildly from consolidation and air bronchograms to solid and subsolid nodules and masses with a bronchogenic distribution. Both unifocal and multifocal forms of the disease show a lower lobe predominance. Like other lepidic predominant neoplasms these tumors often appear radiologically as ground glass opacities, therefore these tumors are sometimes difficult to differentiate from inflammatory infiltrates in CT scans.

Histopathology: These tumors show a predominantly lepidic growth pattern but often also have the same heterogeneous mixture also including acinar, papillary, micropapillary, and solid growth as in nonmucinous tumors. In some tumor areas the basic structure of the lung is destroyed. The tumor cells are columnar, with elongated hyperchromatic nuclei. Tumor cells show significant intracytoplasmic, mostly apically located mucus. Alveolar spaces often contain mucin. When stromal invasion is seen, the malignant cells may show less cytoplasmic mucin and more atypia. . There is a strong tendency for multicentric, multilobar, and bilateral lung involvement, which may reflect aerogenous spread. Lymph node and distant metastases rarely occur. Because cytologic atypia is usually inconspicuous or absent in IMAs, definitive diagnosis of malignancy via biopsy is frequently challenging. In transbronchial biopsy, accurate targeting could be limited since most IMAs are located in the periphery of lower lobes. Moreover, submucosal mucinous glands of bronchial tissue and the tumor cells of IMA could mimic each other because of bland-looking cytomorphology and intracytoplasmic mucin. Percutaneous computer tomography (CT)-guided lung biopsy appears to be more effective way to obtain the diagnostic tissue, however biopsied specimen could be composed of acellular mucin pool only since the alveolar spaces at the tumor periphery are often filled with mucin, which may correspond to the lobar pneumonia-like area on the chest CT image. Even if tumor cells are

included in the specimen, a small amount of mucinous cells with bland morphology could be insufficient to make a definitive diagnosis of malignancy.

Immunohistochemistry: By immunohistochemistry these tumors frequently show an expression of CK 7 and may co-express CK20 and CDX2. HNF4α and GATA6 has recently been described in MIA but specificity seems to be low. TTF1 and Napsin A as well as SPA are often negative. Recently HNF4α and GATA6 has been described but these markers are not highly specific.

Molecular pathology: KRAS is the most common mutation (60 %). Interestingly, codon p.G12D and p.G12V similarly to GI carcinomas are most frequently involved. Unlike in non-mucinous adca EGFR mutations are rare (1 %). Oncogenic fusions are mutually exclusive with KRAS mutations and occur in 12 % of cases. The most common fusion involve NRG1, followed by ALK, ERBB2, ERBB4, BRAF, RERT, ROS1 and NTRK1.

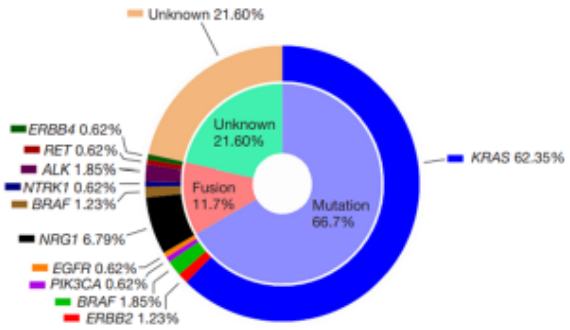

Figure 2 Pie chart showing the percentages of invasive mucinous adenocarcinomas (n=162) that harbor the indicated driver genes [combined data from references (14) and (15) are shown].

Staging: Size determination for TNM classification include the lepidic pattern in this type of tumor and this differs from the situation in non-mucinous carcinomas where only invasive component is included.

Prognosis: The prognosis of IMA is not well-characterized but some recent studies indicate a more favorable outcome with regard to DFS and OS than INMA's. The pneumonic-type of distribution seem to be more aggressive than the solitary-type.

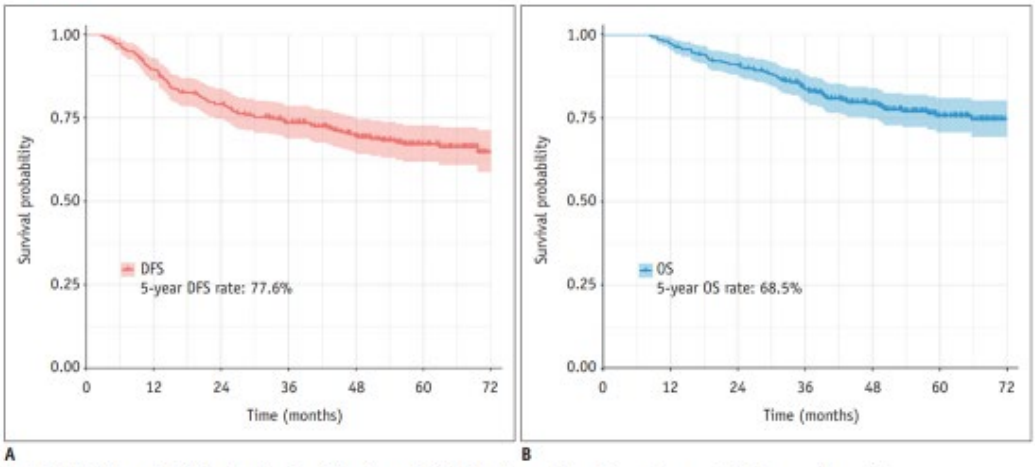

Fig. 2. DFS (A) and OS (B) of patients with primary IMA of the lung. DFS = disease-free survival, OS = overall survival

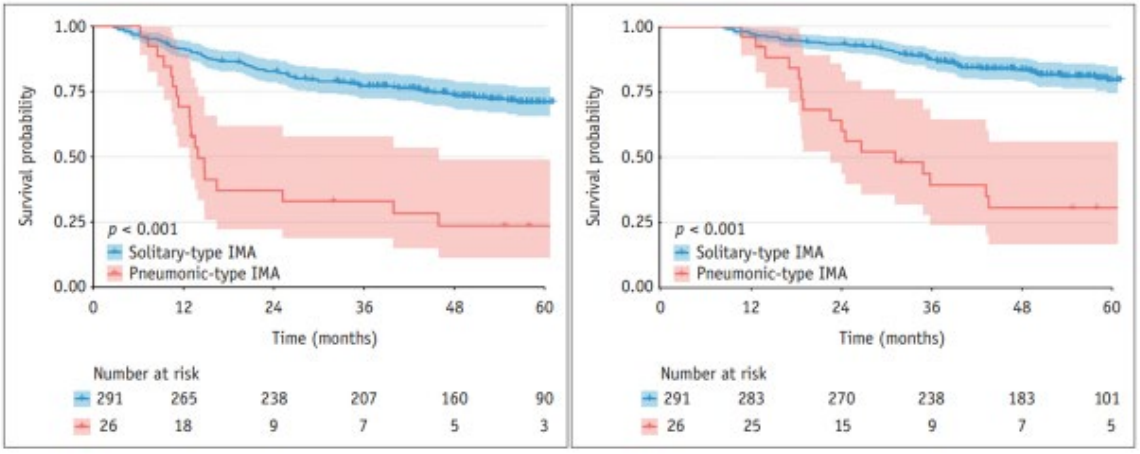

CD74-NRG1: A novel somatic gene fusion, *CD74–NRG1* was discovered in IMA's in 2014. Mechanistically, *CD74–NRG1* leads to extracellular expression of the EGF-like domain of NRG1 III-β3, thereby providing the ligand for ERBB2–ERBB3 receptor complexes. Thus, *CD74–NRG1* gene fusions are activating genomic alterations in invasive mucinous adenocarcinomas that may represent a therapeutic opportunity for invasive mucinous lung adenocarcinomas, a tumor with no effective treatment that frequently presents with multifocal unresectable disease.

NRG1 fusions are present in multiple cancer types, and in a high proportion of lung IMA. Recent NRG1 registry data indicate that a substantial proportion (20%) of NRG1 fusion-positive NSCLC cases are nonmucinous adenocarcinomas. Other NRG1-positive tumor types include pancreatic cancer, gallbladder cancer, renal cell carcinoma, bladder cancer, ovarian cancer, breast cancer, neuroendocrine tumor, sarcoma, and colorectal cancer.

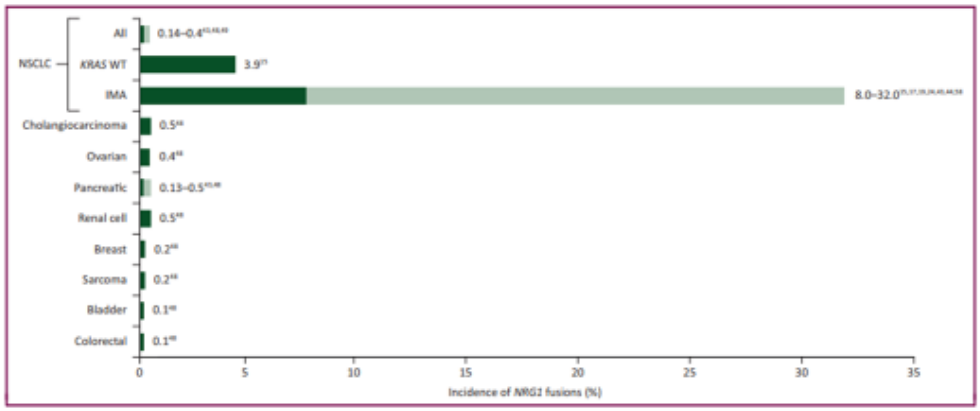

Figure 2. Incidence of *NRG1* fusions in cancer.
IMA, invasive mucinous adenocarcinoma; *KRAS* WT, Kirsten rat sarcoma viral oncogene homolog wild-type; NSCLC, non-small-cell lung cancer. *Note:* For pancreatic cancer, where reported (Jonna et al. (2019)[65]), all cases were KRAS WT.

Differential diagnosis of mucinous tumors in the lung: The list of lung tumors with mucinous features in the present WHO classification (WHO 5th ed) is long and the definitions between various diagnoses are sometimes difficult and vague.

- Bronchiolar adenoma
- Mucinous cystadenoma
- Mucous gland adenoma
- AAH mucinous (not in WHO)
- AIS mucinous
- MIA mucinous
- Lepidic predominant adenocarcinoma mucinous
- IMA
- Colloid adenocarcinoma
- Fetal-type adenocarcinoma
- Enteric-type adenocarcinoma
- Adenosquamous carcinoma
- Non-mucinous invasive adenocarcinomas
- Various salivary gland type tumors including mucoepidermoid carcinoma

- Metastasis from intrapulmonary mucinous adenocarcinoma
- Metastasis from extrapulmonary mucinous adenocarcinoma

Conclusions:

- IMA seem to have unique histological, immunohistochemical, molecular and clinical characteristics
- Our rapidly evolving knowledge of the genetic and clinical characteristics of IMAs confirms the uniqueness of this disease among other primary lung adenocarcinomas
- Via comprehensive clinicopathologic and molecular analyses, IMAs will be more accurately diagnosed and more thoroughly investigated.
- Prognostically unfavorable patterns like pneumonia-like presentation occur and can delay diagnosis with high stage presentation at diagnosis as consequence
- CD74-NRG1 fusion is common and characteristic for this tumor and offer some chance of targeting therapy
- New findings regarding the targetable genetic alterations and clinical profiles of IMAs are anticipated to result in better patient management
- Lung cancer classification of carcinomas with mucin production is evolving but still sometimes difficult to apply to individual cases

References:

1. Cha YJ, Shim HS. Biology of invasive mucinous adenocarcinoma of the lung. Transl Lung Cancer Res. 2017 Oct;6(5):508-512.
2. Lambe G, Durand M, Buckley A, Nicholson S, McDermott R. Adenocarcinoma of the lung: from BAC to the future. Insights Imaging. 2020 May 19;11(1):69.
3. Fernandez-Cuesta L, Plenker D, Osada H, Sun R, Menon R, Leenders F, Ortiz-Cuaran S, Peifer M, Bos M, Daßler J, Malchers F, Schöttle J, Vogel W, Dahmen I, Koker M, Ullrich RT, Wright GM, Russell PA, Wainer Z, Solomon B, Brambilla E, Nagy-Mignotte H, Moro-Sibilot D, Brambilla CG, Lantuejoul S, Altmüller J, Becker C, Nürnberg P, Heuckmann JM, Stoelben E, Petersen I, Clement JH, Sänger J, Muscarella LA, la Torre A, Fazio VM, Lahortiga I, Perera T, Ogata S, Parade M, Brehmer D, Vingron M, Heukamp LC, Buettner R, Zander T, Wolf J, Perner S, Ansén S, Haas SA, Yatabe Y, Thomas RK. CD74-NRG1 fusions in lung adenocarcinoma. Cancer Discov. 2014 Apr;4(4):415-22.
4. Cheema PK, Doherty M, Tsao MS. A Case of Invasive Mucinous Pulmonary Adenocarcinoma with a CD74-NRG1 Fusion Protein Targeted with Afatinib. J Thorac Oncol. 2017 Dec;12(12):e200-e202.
5. Nakagomi T, Goto T, Hirotsu Y, Shikata D, Yokoyama Y, Higuchi R, Otake S, Amemiya K, Oyama T, Mochizuki H, Omata M. Genomic Characteristics of Invasive Mucinous Adenocarcinomas of the Lung and Potential Therapeutic Targets of B7-H3. Cancers (Basel). 2018 Nov 30;10(12):478.
6. Laskin J, Liu SV, Tolba K, Heining C, Schlenk RF, Cheema P, Cadranel J, Jones MR, Drilon A, Cseh A, Gyorffy S, Solca F, Duruisseaux M. NRG1 fusion-driven tumors: biology, detection, and the therapeutic role of afatinib and other ErbB-targeting agents. Ann Oncol. 2020 Dec;31(12):1693-1703.
7. Kim M, Hwang J, Kim KA, Hwang S, Lee HJ, Jung JY, Lee JG, Cha YJ, Shim HS. Genomic characteristics of invasive mucinous adenocarcinoma of the lung with multiple pulmonary sites of involvement. Mod Pathol. 2021 Jul 21.
8. Cow CH, Hsieh MS, Liu YN, Lee YH, Shih JY. Clinicopathological Features and Survival Outcomes of Primary Pulmonary Invasive Mucinous Adenocarcinoma. Cancers (Basel). 2021 Aug 15;13(16):4103.
9. Wang T, Yang Y, Liu X, Deng J, Wu J, Hou L, Wu C, She Y, Sun X, Xie D, Chen C. Primary Invasive Mucinous Adenocarcinoma of the Lung: Prognostic Value of CT Imaging Features Combined with Clinical Factors. Korean J Radiol. 2021 Apr;22(4):652-662.

10. Maasdorp SD. Wolf in sheep's clothes: An uncommon case of pneumonic-type adenocarcinoma. Afr J Thorac Crit Care Med. 2021 Mar 9;27(1):10.7196/AJTCCM.2021.v27i1.048.
11. Popper HH. Cons: the confusing mucinous adenocarcinoma classification. Transl Lung Cancer Res. 2017 Apr;6(2):234-240.

AMR SEMINAR #78
CASE 15

Contributed by: Luca DeTommasso, M.D., Humanitas University, Italy.

Case history. A 69-year-old man with a previous history of prostatic cancer (2013) presented with anaemia and dyspnoea. The patient underwent a colon biopsy that allowed a diagnosis of adenocarcinoma of the colon. A CT scan revealed a 6 cm mass in the anterior mediastinum, highly suspicious for thymoma. The patient then underwent right colectomy (with a conclusive diagnosis of adenocarcinoma of the colon G3 pT3 pN0) and a resection of the mediastinal mass.

Pathological Findings. On cut section, the mass measured 6 cm. in greatest axis, showed well defined margins and was composed of whitish tissue arranged in fascicles. At histology the lesion was characterized by spindle cells arranged in bundles with some alternating myxoid and hyalinized areas. Neoplastic cells showed positive reactivity with MUC4 and EMA. Other markers (SMA, desmin, CD34. S100, mdm2) were consistently negative. Molecular analysis showed EWSR1 rearrangement; FUS was not translocated.

Diagnosis: Primary low grade fibromyxoid sarcoma (LGFMS) of the mediastinum.

Comment: In 1987, Evans first recognized LGFMS as a unique entity affecting mainly middle-aged adults, presenting as a slow-growing, asymptomatic tumor with deceivingly mild histology but with a higher risk of recurrence and metastasis. In 1999, Takanami et al reported the first case of mediastinal LGFMS in a 35-year-old male. The majority of LGFMSs have a recurrent balanced translocation between chromosomes 7 and 16, which results in the union of 'Fused in Sarcoma' RNA binding protein' (FUS) and the CREB3L2 gene. Translocation of 'FUS-CREB3L1' fusion gene is reported in about 5% of the LGFMS cases. EWSR1 gene can replace FUS in occasional examples of LGFMS. The partner gene is CREB3L1, rather than the more usual CREB3L2. Although FISH for FUS gene rearrangement is negative in these tumours, positive immunohistochemistry for MUC4 remains of diagnostic value.

References:

- Evans HL. Am J Clin Pathol. 1987; 88:615–9.
- Takanami I, et al. J Thorac Cardiovasc Surg. 1999; 118:970-1.
- Lau PP, et al. Am. J. Surg. Pathol. 2013; 37; 734– 738.

AMR SEMINAR #78
CASE 16

Contributed by: Daniel D. Wong, M.D., Queen Elizabeth II Medical Center, Australia.

Clinical History: 32 year old female, previously well, with palpable left pubic lump. MRI showed a 39 x 36 x 22mm subcutaneous mass in the left inguinal region, T2 hyperintense, T1 isointense to muscle and with heterogeneous enhancement. The mass showed moderate to high FDG-avidity on PET, with no distant metastatic disease. There is no recurrence on surveillance imaging 2 years post-resection.

Macroscopic Features: The tumor was excised with a margin of normal tissue (following an FNA suggesting a diagnosis of "myoepithelioma-like tumor of the vulvar region"). The excision showed a circumscribed, lobulated and soft hemorrhagic mass confined to the subcutis, 40 x 40 x 25mm. There was no connection to the overlying skin.

Histological, Immunohistochemical and Molecular Genetic Findings: The tumor formed a circumscribed, lobulated and thinly encapsulated mass within subcutaneous fat. There was a distinctly biphasic appearance, consisting of a dominant lower grade epithelioid component (80%) and a smaller high-grade round cell component (20%).

The former showed a spectrum of growth patterns. For the most part, large rounded epithelioid and rhabdoid cells occurred in islands, nests and cords, set in a myxoid and hyalinized stroma. The cells displayed moderately pleomorphic nuclei with finely granular chromatin, variably prominent nucleoli and abundant eosinophilic cytoplasm. Mitoses numbered up to 12 per 10 HPF in this component. The cells stained diffusely for EMA, smooth muscle actin and CD99 (membranous), with patchy co-expression of ER and only focal (<10%) staining for AE1/AE3 and CK8/18. Negative markers included CK7, CK20, S100, GFAP, h-caldesmon, desmin and CD34. There was diffuse loss of INI1 (SMARCB1).

Juxtaposed was a high-grade round cell component composed of sheets of small round cells, sometimes forming pseudo-rosettes. Mitotic activity was prominently increased in this region, with >50 mitoses counter per 10 HPF and with focal necrosis. There was no vascular invasion. These cells were negative for all markers above, with the exception of diffuse staining for synaptophysin, with isolated expression of AE1/AE3 and focal staining for smooth muscle actin. INI1 (SMARCB1) was diffusely lost again.

Interphase FISH studies showed no rearrangement of *EWSR1, FUS* and *NR4A3*.

Diagnosis: Malignant myoepithelioma of soft tissue or myoepithelioma-like tumor of the vulvar region (MELTVR), with transformation to high-grade round cell malignancy.

Comment: This case shows features compatible with malignant myoepithelioma of soft tissue, although with unusual transformation to a high-grade round cell malignancy. The latter

demonstrates scattered pseudo-rosettes and diffuse synaptophysin expression suggesting neuroectodermal differentiation. Whilst myoepithelioma is characterized by a spectrum of growth patterns and cytomorphology, this pattern of transformation is not well recognized. Round cell morphology has been previously reported,[1, 2] although not as a pattern of transformation from a lower grade component and without neuroectodermal features. The appearances here are more akin to what has been described as "dedifferentiation" in a single case of malignant myoepithelioma of the parotid gland back in 2003.[3]

This case is of further interest in that it may, more specifically, represent an example of transformation in "myoepithelioma-like tumor of the vulvar region (MELTVR)," an entity first proposed by Yoshida *et al*. in 2015.[4] These rare tumors occur in the subcutis of the vulva and surrounding regions of adult women (median 41 years), showing benign/locally aggressive behavior when adequately excised.
MELTVR shares morphological and some immunohistochemical features with soft tissue myoepithelioma and their exact nosological relationship is yet to be fully determined. However, MELTVR appears to have gained acceptance as a distinct entity with multiple case reports published since the original series.[5-7] The lower grade component of the current case displays many of the features proposed as being distinctive to this entity, namely:

- Complete absence of S100 and GFAP (positive staining typically seen in conventional soft tissue myoepithelioma and considered definitional by some[8-10])
- Only focal staining for keratins (many, but not all, cases in the original series were completely negative[4])
- Diffuse staining for EMA and ER
- Diffuse loss of INI1 (SMARCB1) expression
- Absence of *EWSR1* rearrangement (seen in up to 50% of soft tissue myoepitheliomas[8]).

If this case does represent MELTVR, the transformation to a high-grade round cell malignancy is a novel finding. Nuclear atypia, mitotic activity of up to 12 per 10 HPF and necrosis were reported in some cases in the original series (all alive without metastases at mean follow-up of 66 months),[4] although in the context of conventional morphological features resembling myoepithelioma and quite unlike the transformation to frankly high-grade round cell areas as seen here (>50 mitoses per 10 HPF and Ki67 proliferation of 80%).
The possibility of proximal-type epithelioid sarcoma was also considered in this case given the presence of rhabdoid cells and diffuse loss of INI1 expression, although the high-grade round cell areas, only focal staining for keratins and absence of CD34 were thought not to be typical for this diagnosis.

Figure Captions:
A. MRI showing lobulated mass in subcutis of left pubic region. **B.** Dominant lower grade component showing epithelioid cells in nests and myxoid stroma. **C.** Transformation to high-grade round cell component with pseudo-rosettes. **D, E.** EMA and ER staining of lower grade component, with loss in transformed areas. **F.** Diffuse INI1 loss. **G.** Focal expression of CK8/18 in lower grade area (<10% of overall section). **H.** Markedly increased Ki67 labelling in transformed round cell component.

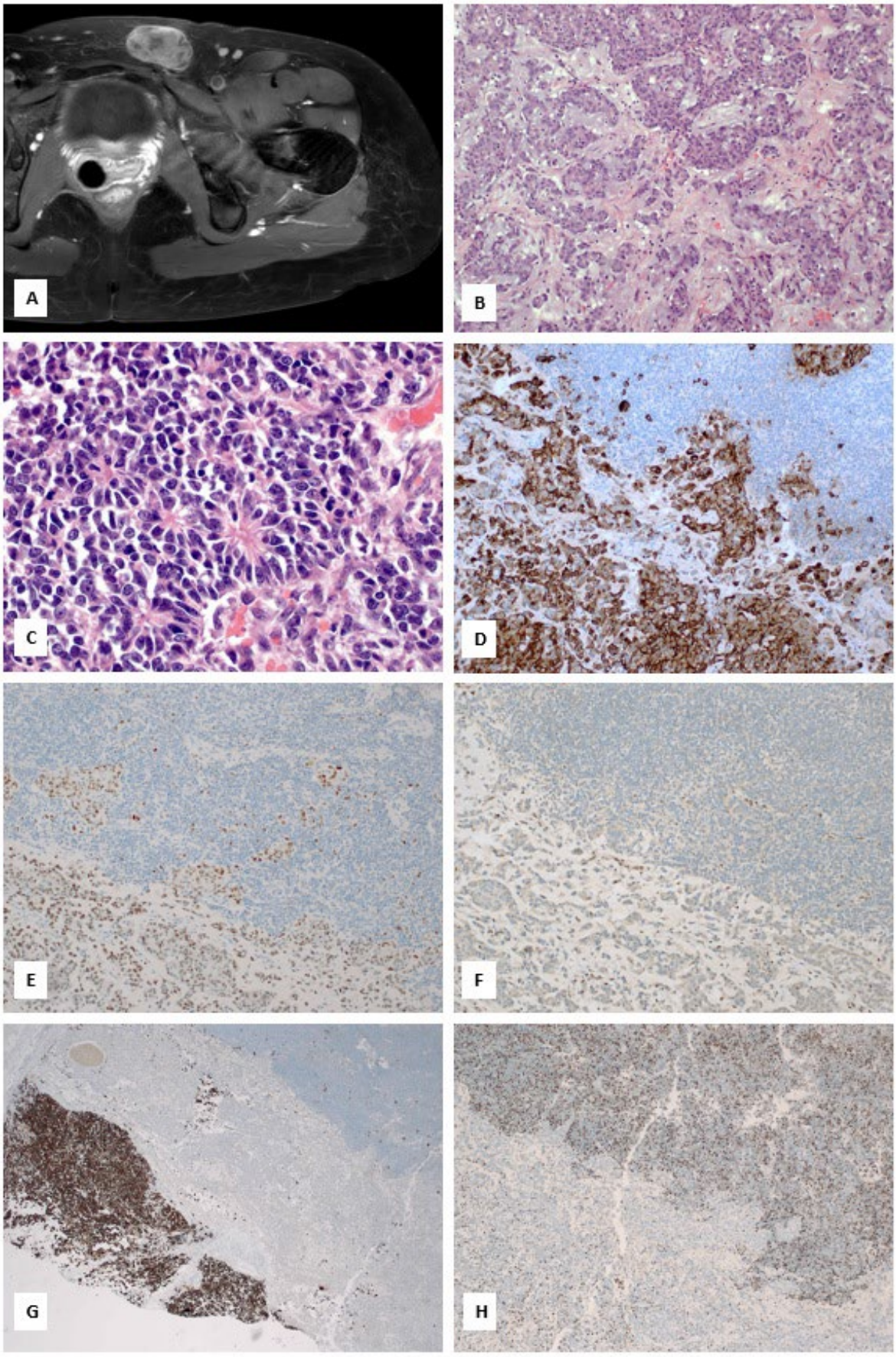
A
B
C
D
E
F
G
H

References:

1. Leckey BD, Jr., John I, Reyes-Mugica M, et al. EWSR1-ATF1 Fusion in a Myoepithelial Carcinoma of Soft Tissue With Small Round Cell Morphology: A Potential Diagnostic Pitfall. *Pediatr Dev Pathol*. 2021; 24: 258-63.
2. El-Kabany M, Al-Abdulghani R, Ali AE, et al. Soft tissue high grade myoepithelial carcinoma with round cell morphology: report of a newly described entity with EWSR1 gene rearrangement. *Gulf J Oncolog*. 2011: 73-7.
3. Ogawa I, Nishida T, Miyauchi M, et al. Dedifferentiated malignant myoepithelioma of the parotid gland. *Pathol Int*. 2003; 53: 704-9.
4. Yoshida A, Yoshida H, Yoshida M, et al. Myoepithelioma-like Tumors of the Vulvar Region: A distinctive Group of SMARCB1-deficient Neoplasms. *Am J Surg Pathol*. 2015; 39: 1102-13.
5. Lin YS, Parasyn A, Paulus F, et al. Myoepithelioma-like tumour of the vulval region: A case report. *Australas J Dermatol*. 2022; 63: e52-e55.
6. Liu X, Chen L, Zhou Q, et al. Myoepithelioma-like tumors of the vulvar region: A case report and review of the literature. *J Obstet Gynaecol Res*. 2022; 48: 2015-20.
7. Zhang HZ, Wang SY. Myoepithelioma-like tumour of the vulvar region. *Pathology*. 2019; 51: 665-68.
8. Antonescu CR, Zhang L, Chang NE, et al. EWSR1-POU5F1 fusion in soft tissue myoepithelial tumors. A molecular analysis of sixty-six cases, including soft tissue, bone, and visceral lesions, showing common involvement of the EWSR1 gene. *Genes Chromosomes Cancer*. 2010; 49: 1114-24.
9. Michal M, Miettinen M. Myoepitheliomas of the skin and soft tissues. Report of 12 cases. *Virchows Arch*. 1999; 434: 393-400.
10. Suurmeijer AJH, Dickson BC, Swanson D, et al. A morphologic and molecular reappraisal of myoepithelial tumors of soft tissue, bone, and viscera with EWSR1 and FUS gene rearrangements. *Genes Chromosomes Cancer*. 2020; 59: 348-56.

AMR SEMINAR #78
CASE 17

Contributed by: Israa Laklouk M.D.

Clinical History: A 28-year-old woman had a multinodular goiter. Ultrasound showed multiple nodules on her thyroid, with two dominant nodules on the left side and one on the right. The patient underwent a fine-needle aspiration (FNA) biopsy of the three largest nodules. The biopsy results indicated that the upper nodule on the right side was benign, the upper nodule on the left side was inconclusive (follicular lesion of undetermined significance - FLUS), and the lower nodule on the left side was non-diagnostic. As the FNA were inconclusive, so she underwent a total thyroidectomy. Intraoperative impression a multinodular goiter without evidence of malignancy.

Gross Description: The total thyroid weight is 36 grams [figure 1A], consisting of a right lobe measuring 5.5 x 3.7 x 3.0 cm and a left lobe measuring 4.6 x 3.5 x 2.1 cm. Upon sectioning the specimen, there are diffusely nodular cut surfaces with a small amount of brown tissue. The nodules vary in size from 0.2 cm to 3.4 cm and have a brown color with some areas of bleeding. In the left lobe, there is solid nodule that are tan-white and well-defined/encapsulated. The entire thyroid tissue was submitted for microscopic examination.

Pathological Findings: The sections reveal that the majority of the thyroid tissue has been replaced by multiple nodules, ranging in size from 0.1 cm to 3.4 cm, which are well-defined and clearly distinguishable from the surrounding non-lesional tissue. In the left lobe, there is a distinct 2.2 cm nodule with a different appearance (a recut slide of this area has been provided). This tumor is clearly demarcated from the non-neoplastic tissue by a thick fibrous capsule and displays a follicular growth pattern with focal solid areas. There are scattered abnormal nuclear features resembling papillary thyroid carcinoma (PTC), as well as oncocytic cytoplasm. Immunohistochemistry staining for BRAF V600E was negative, indicating the absence of a specific genetic mutation associated with PTC.

Considering the patient's young age and the presence of multiple edematous nodules in the multinodular thyroid, these findings suggest the possibility of PTEN hamartoma tumor syndrome. As a result, PTEN immunohistochemistry staining was performed. The staining revealed the absence of PTEN expression in the adenomatous nodules (Figure 1 C and D) as well as in the PTC (Figure 2 D), while the adjacent non-lesional thyroid follicles and intralesional endothelial cells showed intact PTEN expression.

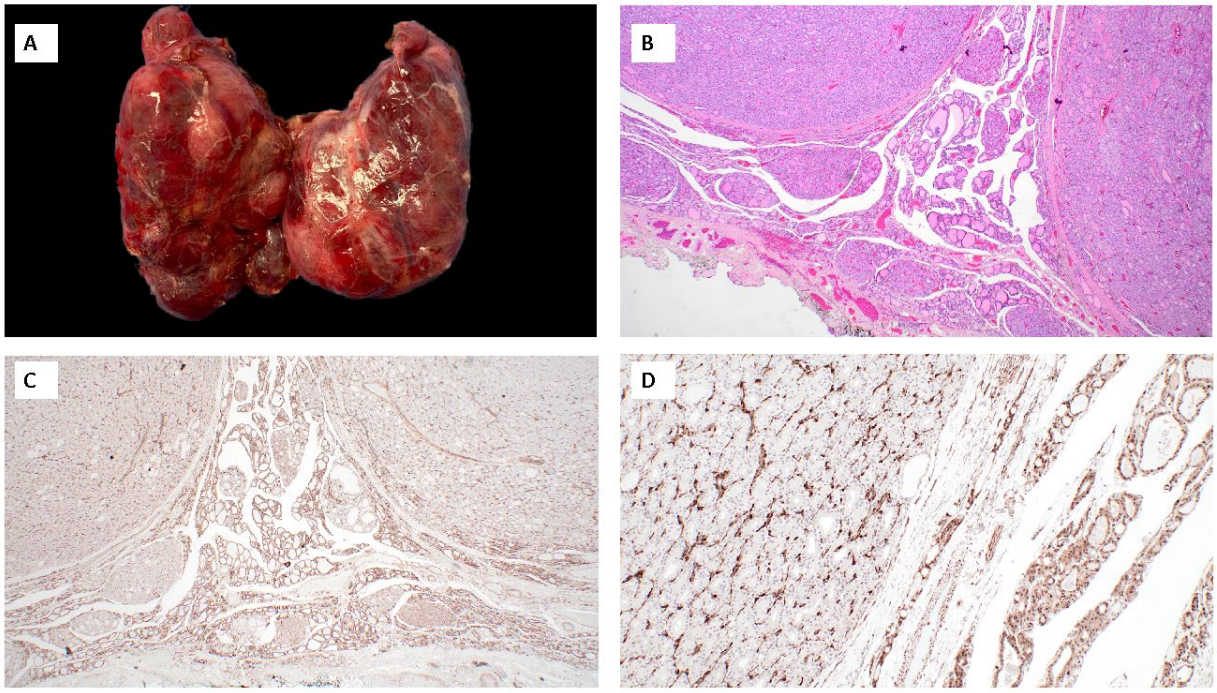

Figure 1: Total thyroidectomy shows a multinodular goiter (A). H&E section shows numerous adenomatous nodules with minimal normal thyroid parenchyma (B). PTEN immunohistochemistry staining reveals the absence of PTEN expression in adenomatous nodules, whereas adjacent non-lesional thyroid follicles and intralesional endothelial cells show intact PTEN expression (C and D).

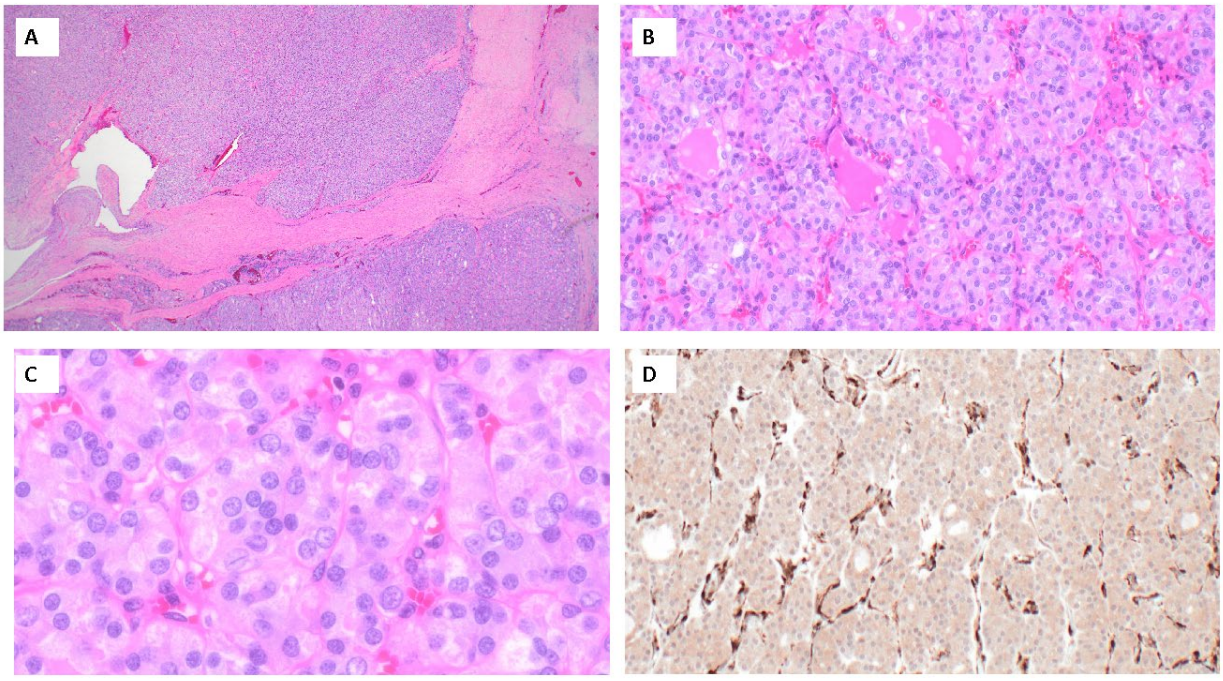

Figure 2: Left lobe upper nodule. Low-power view showing capsular invasion in an encapsulated follicular variant of papillary thyroid carcinoma (A). Medium-power view shows compacted and collapsed follicles (B). High-power view shows PTC nuclear atypia (C).PTEN

immunohistochemistry staining shows the absence of PTEN expression in thyroid carcinoma, while the expression remains intact in the endothelial cells within the lesion (D).

Diagnosis: Invasive encapsulated follicular variant of papillary thyroid carcinoma (IEFVPTC), and numerous adenomatous nodules with PTEN loss

Comments:

1. I am presenting this case because the appearance of the thyroid gland is atypical and differs from what is commonly observed in multinodular goiter. However, the histological features are consistent with thyroid neoplasms associated with PTEN mutation.
2. The final pathology results confirm the presence of multiple adenomatous nodules, along with an encapsulated follicular variant of papillary thyroid carcinoma (PTC) that shows loss of PTEN expression on immunocytochemistry. Upon reviewing the patient's detailed clinical history it was discovered that she had previous occurrences of multiple breast fibroadenomas and a uterine leiomyoma.
3. Given the patient's young age, multinodular thyroid with PTEN loss confirmed by immunocytochemistry, and previous history of multiple breast fibroadenomas and uterine leiomyoma, the findings suggest the possibility of PTEN hamartoma tumor syndrome. The patient was referred for genetic testing, which confirmed the presence of a germline mutation in the PTEN gene.
4. Recognition of Cowden syndrome (CS) or PTEN hamartoma tumor syndrome (PHTS) is crucial for initiating cancer screening and providing genetic counseling. Therefore, immunohistochemical staining for PTEN can help identify CS/PHTS in patients with multiple adenomatous thyroid nodules. The National Comprehensive Cancer Network (NCCN) has incorporated the revised clinical criteria for PTEN hamartoma syndrome into its 2.2021 CS/PTEN hamartoma syndrome management guidelines, serving as a basis for determining the need for genetic testing for PTEN mutation.

References:

- Barletta JA, Bellizzi AM, Hornick JL. Immunohistochemical staining of thyroidectomy specimens for PTEN can aid in the identification of patients with Cowden syndrome. Am J Surg Pathol. 2011 Oct;35(10):1505-11. doi: 10.1097/PAS.0b013e31822fbc7d. PMID: 21921783.
- Laury AR, Bongiovanni M, Tille JC, Kozakewich H, Nosé V. Thyroid pathology in PTEN-hamartoma tumor syndrome: characteristic findings of a distinct entity. Thyroid. 2011 Feb;21(2):135-44. doi: 10.1089/thy.2010.0226. Epub 2010 Dec 29. PMID: 21190448

AMR SEMINAR #78
CASE 18

Contributed by: Anais Malpica, M.D., M.D. Anderson Cancer Center.

Clinical History: A 52 year-old female presented with lower abdominal pain and a palpable mass. Imaging studies showed a 17 cm, left ovarian multicystic mass with focal nodularity in one of the cysts wall. The patient underwent a total abdominal hysterectomy with bilateral salpingo-oophorectomy, appendectomy, omentectomy and multiple peritoneal biopsies. The tumor was FIGO stage 1A. The patient received 5 cycles of adjuvant chemotherapy (oxaliplatin, capecitabine and avastin) and after a follow-up of 7 years she has no evidence of disease.

Pathologic findings: The tumor was multicystic, with abundant mucin and measured 19 cm. An ill-defined area of nodularity was noted. IHC studies (CK7 patchy positive, CK20 patchy positive in the mucinous borderline component; pan-keratin and EMA positive in the anaplastic component).

Diagnosis: Anaplastic carcinoma in a mucinous borderline tumor.

Discussion:
Anaplastic carcinoma arising in ovarian mucinous tumors is an uncommon neoplasm. It occurs in patients with a wide age range, 15- 93 years (mean 44), who present with symptoms related to the ovarian mass. The tumor is usually unilateral and detected as a large, multicystic mucinous neoplasm (mean size, 20 cm). The anaplastic carcinoma can appear as a single nodule or multiple nodules. Histologically, it can be rhabdoid, spindle or pleomorphic while the associated mucinous tumor can be a mucinous borderline tumor or an invasive mucinous carcinoma. The cells of anaplastic carcinoma are typically positive for keratin, although a rare case has been negative for this marker and the diagnosis has been based on the overexpression of p53. Claudin 4 may be positive or negative. More recently, it has been found that 36% of anaplastic carcinomas arising in mucinous tumors of the ovary and peritoneum may show loss of nuclear staining for any SWI/SNF protein (SMARCA4, SMARCA2, SMARCB1 and ARID1A). Interestingly, the loss of any of these proteins appears to be more frequent in tumors with a rhabdoid appearance. Most patients with this neoplasm have disease limited to the ovary, either FIGO stage 1A or 1C. Patients with disease FIGO stage 1A appear to have a favorable outcome.

References:

- Provenza C, Young RH, Prat J. Anaplastic carcinoma in mucinous ovarian tumors: a clinicopathologic study of 34 cases emphasizing the crucial impact of stage on prognosis, their histologic spectrum, and overlap with sarcomalike mural nodules. Am J Surg Pathol. 2008 Mar;32(3):383-9.

- Nakamura E, Shimizu M, Mikami Y, Kawai J, Manabe T. Ovarian mucinous cystadenocarcinoma with malignant mural nodules. Pathol Int. 1998 Aug;48(8):645-8.
- Chaudet K, Kem M, Lerwill M, Young RH, Mino-Kenudson M, Agaimy A, McCluggage WG, Oliva E. SWI/SNF protein and claudin-4 expression in anaplastic carcinomas arising in mucinous tumours of the ovary and retroperitoneum. Histopathology. 2020 Aug;77(2):231-239.

AMR SEMINAR #78
CASE 19

Contributed by: Preetha Ramalingam, M.D., M.D. Anderson Cancer Center.

Clinical History:
A 62-year-old female with history of breast cancer and on Tamoxifen therapy presented with abnormal uterine bleeding. Ultrasound showed thickened endometrium and an incidental 12 cm right adnexal mass. Endometrial biopsy showed atypical hyperplasia. The patient underwent total abdominal hysterectomy and bilateral salpingo-oophorectomy.

Immunohistochemical studies:
CD10 +, SF1 +, WT1+, β-catenin nuclear staining, inhibin negative, calretinin negative.

Diagnosis: Microcystic stromal tumor of ovary.

Discussion:
Microcystic stromal tumor (MCST) is an uncommon ovarian neoplasm, initially described by Irving and Young in 2009.[1] In the *World Health Organization Classification of Tumors of* Female Genital Tumors,[2] this neoplasm is included in the pure stromal category of the sex-cord stromal tumors.
The tumors present in a wide age range (23 to 71 years) with a mean age of 45 years. The most common presentation is with symptoms related to a pelvic mass, and hormonal manifestations are usually absent. Mutations in either *CTNNB1* gene or the *APC* gene resulting in activation of the Wnt/β-catenin pathway have been reported in these tumors.[3,4] MCSTs may be associated with familial adenomatous polyposis (FAP) and represent extracolonic manifestation.[5,6] The tumors are unilateral with a mean size of ~9 cm. Grossly, the cut surface is typically solid, firm with a tan-white appearance. Cystic change or hemorrhagic foci may be present. The triad of histologic features include microcysts, solid cellular areas, and intersecting fibrous stroma. The cells usually have bland nuclei, that are round to oval or spindled, with fine chromatin and indistinct nucleoli. Mitotic index is typically low. Foci of bizarre nuclei can be found, and in some cases this feature may represent a prominent histologic component.[7]
Immunohistochemically, the tumor is typically positive for CD10, WT1, cyclin D1, and SF1, while negative for EMA, inhibin, and calretinin. While androgen receptor may be positive, the tumor cells are invariably negative for ER and PR. As a result of mutations in genes associated with Wnt/β-catenin pathway, the tumors show characteristic nuclear expression/localization of β-catenin by immunostains, which facilitates the diagnosis.[3,4] The majority of MCST have been reported to have an indolent clinical course, however, a few cases were reported with late recurrence (~9 yrs after diagnosis), [8,9] and with omental metastasis at presentation[10]. The current patient is without evidence of disease 5-yrs post-surgery. As the histologic features do not appear to predict outcomes, follow up of these patients may be prudent. Furthermore, given the association with FAP, molecular testing to rule out *APC* gene mutations is recommended.

References:

- Irving JA, Young RH. Microcystic stromal tumor of the ovary: report of 16 cases of a hitherto uncharacterized distinctive ovarian neoplasm. Am J Surg Pathol. 2009 Mar;33(3):367-75. PMID: 18971779.
- Irving JA, Maeda, D. Microcystic stromal tumor. Edited by the WHO Classification of Tumors Editorial Board. Female Genital Tumors. World Health Organization Classification of Tumors, Lyon: IARC Press, 2020; 597-98.
- Irving JA, Lee CH, Yip S, Oliva E, McCluggage WG, Young RH. Microcystic Stromal Tumor: A Distinctive Ovarian Sex Cord-Stromal Neoplasm Characterized by FOXL2, SF-1, WT-1, Cyclin D1, and β-catenin Nuclear Expression and CTNNB1 Mutations. Am J Surg Pathol. 2015 Oct;39(10):1420-6. PMID: 26200099.
- Maeda D, Shibahara J, Sakuma T, Isobe M, Teshima S, Mori M, Oda K, Nakagawa S, Taketani Y, Ishikawa S, Fukayama M. β-catenin (CTNNB1) S33C mutation in ovarian microcystic stromal tumors. Am J Surg Pathol. 2011 Oct;35(10):1429-40. PMID: 21881488.
- Lee SH, Koh YW, Roh HJ, Cha HJ, Kwon YS. Ovarian microcystic stromal tumor: A novel extracolonic tumor in familial adenomatous polyposis. Genes Chromosomes Cancer. 2015 Jun;54(6):353-60. PMID: 25820106.
- McCluggage WG, Irving JA, Chong AS, Clarke BA, Young RH, Foulkes WD, Rivera B. Ovarian Microcystic Stromal Tumors Are Characterized by Alterations in the Beta-Catenin-APC Pathway and May be an Extracolonic Manifestation of Familial Adenomatous Polyposis. Am J Surg Pathol. 2018 Jan;42(1):137-139. PMID: 29076875.
- Pongsuvareeyakul T, Kingnate C, Sukpan K, Khunamornpong S. Microcystic Stromal Tumor with Predominant Bizarre Nuclei of Ovary in a Pregnant Woman. Case Rep Pathol. 2022 Dec 7;2022:8457901. PMID: 36530937.
- Zhang Y, Tao L, Yin C, Wang W, Zou H, Ren Y, Liang W, Jiang J, Zhang W, Jia W, Li F. Ovarian microcystic stromal tumor with undetermined potential: case study with molecular analysis and literature review. Hum Pathol. 2018 Aug; 78:171-176. PMID: 29458068.
- Kojima, N., Yoshida, H., Uno, M. *et al.* Microcystic stromal tumor of the ovary: a recurrent case with somatic *CTNNB1* missense mutation. *Virchows Arch* 481, 799–804 (2022). PMID: 29458068.
- Man X, Wei Z, Wang B, Li W, Tong L, Guo L, Zhang S. Ovarian microcystic stromal tumor with omental metastasis: the first case report and literature review. J Ovarian Res. 2021 May 27;14(1):73. PMID: 34044845.